

FINAL REPORT

Title: Less fuel for the fire: How will drought amplify effects of short-interval fire?

JFSP PROJECT ID: 20-1-01-6

November 2022

Kristin H. Braiunas

University of Wisconsin-Madison

Current address: Technical University of Munich

Monica G. Turner

University of Wisconsin-Madison



FIRESCIENCE.GOV
Research Supporting Sound Decisions



The views and conclusions contained in this document are those of the authors and should not be interpreted as representing the opinions or policies of the U.S. Government. Mention of trade names or commercial products does not constitute their endorsement by the U.S. Government.

Table of Contents

Abstract.....	1
Objectives.....	1
Background	2
Materials and Methods.....	4
Study area.....	4
Reburn and plot selection.....	5
Field data collection	6
Biomass and fuels calculations.....	6
Question 1: Effects of short-interval fire, climate, and other factors on forest recovery.....	6
Question 2: Forest biomass and fuels after short- versus long-interval fire	7
Question 3: Comparing UAS data collection methods and derived forest measurements.....	7
Results and Discussion.....	9
Question 1: Effects of short-interval fire, climate, and other drivers on forest recovery.....	9
Question 2: Forest biomass and fuels after short- versus long-interval fire	11
Question 3: Comparing UAS data collection methods and derived forest measurements.....	16
Discussion	19
Science Delivery	21
Conclusions.....	22
Key Findings.....	22
Management Implications.....	23
Future Research	24
Literature Cited	25
Appendix A: Contact Information for Key Project Personnel.....	A1
Appendix B: Completed/Planned Science Delivery Products.....	B1
Appendix C: Metadata	C1
Appendix D: Supplemental Tables.....	D1

List of Tables

- Table 1: Multiple linear regression models predicting post-fire stem density
Table 2: Comparison of UAS data collection methods
Table D1: Presence and stem density by species of post-fire trees
Table D2: Canopy and surface fuel and biomass pools in long- and short-interval plots

List of Figures

- Figure 1: Study area and site design for paired long- and short-interval plots
Figure 2: General characteristics of plots included in this study
Figure 3: Plot and mission layout for UAS data collection
Figure 4: Comparison of stem density following long- versus short-interval fire
Figure 5: Stem density by species in long- versus short-interval plots
Figure 6: Relationships between stem density and climate or distance to unburned edge

- Figure 7: Biomass and fuels following long- versus short-interval fire
 Figure 8: Illustrative photos of long- and short-interval plot pairs
 Figure 9: Relationships between climate and difference in biomass between paired plots
 Figure 10: Biomass of dead woody fuels by size class
 Figure 11: Aboveground biomass trajectories following long- and short-interval fire
 Figure 12: Comparison of UAS and field measurements for metrics of forest structure
 Figure 13: Comparison of accuracy of different methods of UAS data collection
 Figure 14: Example UAS point clouds highlighted snag versus tree identification
 Figure 15: Potential recovery trajectories for aboveground biomass after stand-replacing fire

List of Abbreviations

- ABLA: *Abies lasiocarpa*, subalpine fir
 BIC: Bayesian Information Criterion
 CBD: Canopy bulk density
 CFL: Canopy fuel load
 DAP: Digital Aerial Photogrammetry
 DBH: Diameter at breast height
 DEM: Digital elevation model
 DWD: Downed woody debris
 GCP: Ground control point
 GPS: Global Positioning System
 GYE: Greater Yellowstone Ecosystem
 PIAL: *Pinus albicaulis*, whitebark pine
 PICO: *Pinus contorta* var. *latifolia*, lodgepole pine
 PIEN: *Picea engelmannii*, Engelmann spruce
 POTR: *Populus tremuloides*, quaking aspen
 PSME: *Pseudotsuga menziesii* var. *glauca*, Douglas-fir
 RGB: Red, green, and blue wavelength
 RGN: Red, green, and near-infrared wavelength
 RMSE: Root-mean-square error
 UAS: Unpersonned aerial system (i.e., drone)
 US: United States
 VPD: Vapor pressure deficit

Keywords

Aspen, biomass, burn severity, driver interactions, fire frequency, forest resilience, Greater Yellowstone, lodgepole pine, reburn, self-regulation, structure from motion photogrammetry, tree regeneration, Unpersonned Aerial System, US Northern Rocky Mountains

Land Acknowledgement

Indigenous peoples including the Crow (Apsáalooke), Shoshone-Bannock, Eastern Shoshone, Blackfeet, Niimiipu (Nez Perce), Salish Kootenai (Flathead), and Aaniiih (Gros Ventre) were killed and forcibly removed from this region during the creation of the national parks. These original inhabitants live in and remain connected to Greater Yellowstone today; restoring and enhancing Native use and governance is important for the future of conservation.

Acknowledgements

Nathan G. Kiel is a co-author on the peer-reviewed manuscript associated with this project. We thank Tania Schoennagel for additional field data. We are grateful for field data collection and scouting assistance from Paul Boehnlein, Nick Tipper, Julia Warren, Diane Abendroth, Olivia Burke, Gunnar Carnwath, Cory Cleveland, Chip Collins, Aidan Cornelison, Todd Erdody, Robbie Heumann, Tyler Hoecker, Paul Hood, Emily Johnson, Timon Keller, Arielle Link, Krista Reicis, Bill Romme, Becky Smith, and Ron Steffens; logistical support from Annie Carlson, Jim Jakicic, Joe Rock, Jim Warren, University of Wisconsin Fleet, Yellowstone National Park Communications Center and Backcountry Rangers, Grand Teton National Park Rangers, and Custer Gallatin National Forest Bozeman Dispatch and Big Timber Work Center; and constructive feedback from John Cataldo, Tristan Goodbody, Brian Harvey, Beckett Hills, and Ojaswee Shrestha. This project has been much improved thanks to comments from Tania Schoennagel, Anthony Ives, Chris Kucharik, Volker Radeloff, and Adena Rissman. We acknowledge funding from a Joint Fire Science Program Graduate Research Innovation award (20-1-01-6) and the University of Wisconsin Vilas Trust. K. Braziunas acknowledges additional support from the International Chapter of the P.E.O. Ventura Neale Trust Endowed Scholar Award, and M. Turner acknowledges support from the National Science Foundation (Award DEB-2027261).

Abstract

As 21st-century climate and fire activity depart from historical baselines, effects on forests are uncertain. Forest managers need to predict and monitor forest recovery and fuel accumulation to anticipate future fire behavior and plan appropriate management activities. We explored how interactions between climate and fire affected post-fire recovery of subalpine forests, which were historically resilient to infrequent (100-300 year) severe fire, in Greater Yellowstone (Northern Rocky Mountains, United States). We sampled paired short- (< 30 year) and long- (> 125 year) interval post-fire plots last burned between 1988 and 2018 to address two questions: (1) *How do short-interval fire, climate, and other factors (topography, distance to live edge) interact to affect post-fire forest recovery?* (2) *How do forest biomass and fuels vary following short- versus long-interval severe fires?* Additionally, a low-cost unpersonned aerial system (i.e., drone) was flown in a subset of post-fire plots to assess: (3) *How do different methods of drone data collection affect derived measurements of forest structure and detection of standing dead snags?* Mean post-fire stem density was an order of magnitude lower following short- versus long-interval fires (3,240 versus 28,741 stems ha⁻¹, respectively). Differences between paired plots increased with greater climate water deficit normal ($\rho = 0.67$) and were amplified at longer distances to live forest edge. Unlike conifers, density of aspen (*Populus tremuloides*), a deciduous resprouter, increased with short- versus long-interval fire (mean 384 versus 62 stems ha⁻¹, respectively). Live biomass and canopy fuels remained low nearly 30 years after short-interval fire, in contrast to rapid recovery after long-interval fire, suggesting that future burn severity may be reduced for several decades following reburns. Short-interval plots also had half as much dead woody biomass compared to long-interval plots (60 versus 121 Mg ha⁻¹), primarily due to the absence of large snags. Measurements derived from drone imagery underestimated tree density in young, dense, post-fire plots but characterized snag and tree height well. The conventional built-in red, green, and blue light sensor outperformed a separate sensor that detected near-infrared reflectance, and ground control points did not improve output accuracy. Overall, our results suggest that a trifecta of short-interval fire, large patch size, and arid post-fire climate could threaten subalpine forest resilience but also reduce future burn severity. These findings could help forest managers prioritize opportunities for management activities or identify areas where forest transitions may be most likely. Identifying reburn locations may be valuable for planning fire suppression activities or identifying potential firefighter access or escape routes. Low cost and standardized approaches make drones a promising technology for collecting forest inventory data.

Objectives

This project used a field data campaign in 16 reburns where recent fire burned subalpine, lodgepole pine forests at both short- (< 30 year, "reburns") and long- (> 125 year) fire return intervals in the Greater Yellowstone Ecosystem (GYE) to address three Joint Fire Science Program task statements: *changing fire environment, fire effects and post-fire recovery, and fuels management and fire behavior*. Forest recovery and fuels were measured in paired short- and long-interval post-fire plots and supplemented with previously collected data ($n = 33$ plot pairs, $n = 66$ total plots) to answer two unresolved questions: (1) *How do short-interval fire, climate, and other factors (topography, distance to live edge) interact to affect post-fire forest recovery?* (2) *How do forest biomass and fuels vary following short- versus long-interval severe fires?* We expected post-fire tree stem densities to be lower in reburns, drier post-fire climate to amplify differences between paired plots, and warmer-drier topographic conditions and greater distance

to live forest edge to decrease post-fire stem density. After short-interval fire, we hypothesized lower loads and delayed recovery of live and dead biomass and fuels. Additionally, a low-cost unpersonned aerial system (UAS) was flown in a subset of post-fire plots to test the viability of using this technology for rapid forest assessment and to collect imagery for science communication. This objective originally focused on comparing different methods of post-processing UAS data (e.g., comparing object-based image identification with regression models) for measuring forest structure in young, often dense, post-fire forests. We modified this objective to instead compare different data collection methods and apply standardized post-processing steps for question (3), *How do different methods of UAS data collection affect derived measurements of forest structure and detection of standing dead snags?* We made this change for a few reasons: due to restrictions on where we were allowed to fly (i.e., not within the National Parks), we were only able to collect data for three plots, limiting our ability to make robust statistical comparisons among approaches; there are now well-documented, standardized approaches for processing UAS imagery and 3D point clouds; and we therefore felt that focusing on data collection would be more relevant to forest managers.

Background

Fires are burning more forested area across the western United States (US) as the climate becomes warmer and drier (Higuera and Abatzoglou 2021). Forests are often resilient, meaning they can absorb disturbance without shifting to a qualitatively different structural or functional state (Holling 1973), under historical patterns of fire activity and when favorable climate enables forest recovery (Johnstone et al. 2016). Fire-adapted traits of tree species (e.g., thick bark, serotinous seed banks, resprouting, and long-distance dispersal; Baker 2009; Pausas and Keeley 2014), together with residual post-fire structures such as dead wood and nearby live seed sources, confer resilience and enable forests to persist or recolonize burned areas (Franklin et al. 2000). However, these disturbance legacies may be lost or diminished under expected changes in fire and climate. For example, more frequent fires may recur before a forest can replenish its former carbon stocks or reach reproductive maturity (Keeley et al. 1999, Turner et al. 2019), larger fires may impair regeneration by increasing distances to seed sources (Harvey et al. 2016a), and more severe fires may facilitate changing post-fire tree species composition by altering soil seedbeds (Johnstone et al. 2010). Tree seedlings are particularly vulnerable to climate change because they tolerate a narrow range of temperature and moisture stress (Jackson et al. 2009, Dobrowski et al. 2015, Hansen and Turner 2019). Simultaneous changes in fire and climate may therefore have amplifying negative effects on post-fire forest recovery.

Projections of future fire often incorporate only climate drivers, but post-fire forest and fuels recovery also affect subsequent fire behavior. In many western US forest landscapes, increasing fire frequency is expected to regulate future fire by decreasing fuel loads, thereby reducing fire spread rates and burn severity (Parks et al. 2014, 2015, Stevens-Rumann et al. 2016, Prichard et al. 2017). These negative feedbacks could counteract the influence of climate on fire at landscape scales (Coop et al. 2020), but may not limit regional climate-driven increases in burning (Abatzoglou et al. 2021). Further, self-regulation after a single severe fire is short-lived in many forest types. For example, lodgepole pine (*Pinus contorta* var. *latifolia*) forests recover fuels rapidly after fire and can burn at similar or higher severity as mature forests within 10-12 years (Harvey et al. 2016b, Nelson et al. 2016, 2017, Braziunas et al. 2022). As climate warms and burned area increases, forest managers need to predict and monitor forest recovery

and fuel accumulation following both short- and long-interval fires to anticipate future fire behavior and plan appropriate management activities.

Critical gaps between fine-scale insights from field studies and coarse-scale trends derived from remotely sensed satellite data make it difficult to quantify mechanisms of forest change over large extents. Low-cost spectral imagery captured by a UAS can bridge the gap between traditional field-based methods and remote sensing platforms by providing high spatial resolution (1 cm or less) optical data and covering spatial extents up to several square kilometers (Senf 2022, Coops et al. 2022). However, researchers must still address knowledge gaps in our understanding of capabilities and limitations of imagery data processing techniques (Digital Aerial Photogrammetry, or DAP) and data collected with UAS (Manfreda et al. 2018). UAS DAP can provide forest managers and researchers with an efficient, cost-effective, and accurate approach for monitoring forests in a future with more fire. UAS may be particularly useful for rapid data collection in areas that are difficult to access.

Short-interval fires (i.e., reburns) are occurring more often, yet understanding of forest and fuels recovery following reburns under a wide range of post-fire climate conditions remains unresolved. In the US Northern Rocky Mountains, 138,061 ha of forest burned twice within a 26-year period (1984-2010), with over one-third of reburns occurring in subalpine forests (Harvey et al. 2016b). High-severity fires in subalpine forests historically recurred every 100-300 years, driven by rare combinations of drought and high wind (Romme and Despain 1989, Whitlock et al. 2008, Higuera et al. 2011), and forests recovered rapidly (Turner et al. 1999). However, area burned is already increasing and climatically based fire rotations could shorten to < 30 years over the 21st century (Westerling et al. 2011). In this study, we used field and UAS data from paired short- and long-interval post-fire plots in Greater Yellowstone that last burned between 1988 and 2018 to ask:

(1) *How do short-interval fire, climate, and other factors (topography, distance to live edge) interact to affect post-fire forest recovery?* We expected post-fire tree stem densities to be lower in short- (< 30-year) compared to long- (> 125-year) interval plots and drier post-fire climate to amplify differences between paired plots (Whitman et al. 2019). We further hypothesized declines in post-fire stem density with warmer-drier topographic conditions and greater distance to live forest edge (Stevens-Rumann and Morgan 2019, Hoecker et al. 2020, Gill et al. 2021).

(2) *How do forest biomass and fuels vary following short- versus long-interval severe fires?* After short-interval fire, we expected lower loads and delayed recovery of live and dead biomass and fuels (Donato et al. 2016, Turner et al. 2019, Stevens-Rumann et al. 2020). In all plots, we expected large fuels (1000-hour downed wood or > 7.6 cm diameter snags) to comprise the majority of dead woody biomass.

(3) *How do different methods of UAS data collection affect derived measurements of forest structure and detection of standing dead snags?* In a subset of three post-fire plots that burned 15 years prior and ranged from low to high tree density, we examined whether using ground control points (GCPs), collecting oblique in addition to nadir imagery, and detecting near-infrared light improved DAP-derived data.

Materials and Methods

Study area

The GYE comprises 89,000 km² (YNP 2017) of mostly federally managed land centered on Yellowstone and Grand Teton National Parks (Figure 1). Greater Yellowstone has cold, snowy winters and mild summers, with most annual precipitation falling as snow. Average summer temperature (1981-2010) is 12.3 °C, and annual precipitation averages 644 mm at centrally located Old Faithful in Yellowstone National Park (WRCC 2021). The region is expected to get warmer and drier over the 21st century, with lengthening fire seasons and harsher conditions for germination and establishment of young tree seedlings (Westerling et al. 2011, Romme and Turner 2015). Since 1950, the GYE has warmed +1.3 °C and annual snowfall has decreased by 25% (Hostetler et al. 2021). Soils are primarily derived from highly infertile, volcanic rhyolite; slightly less infertile andesite; or sedimentary parent materials (Despain 1990).

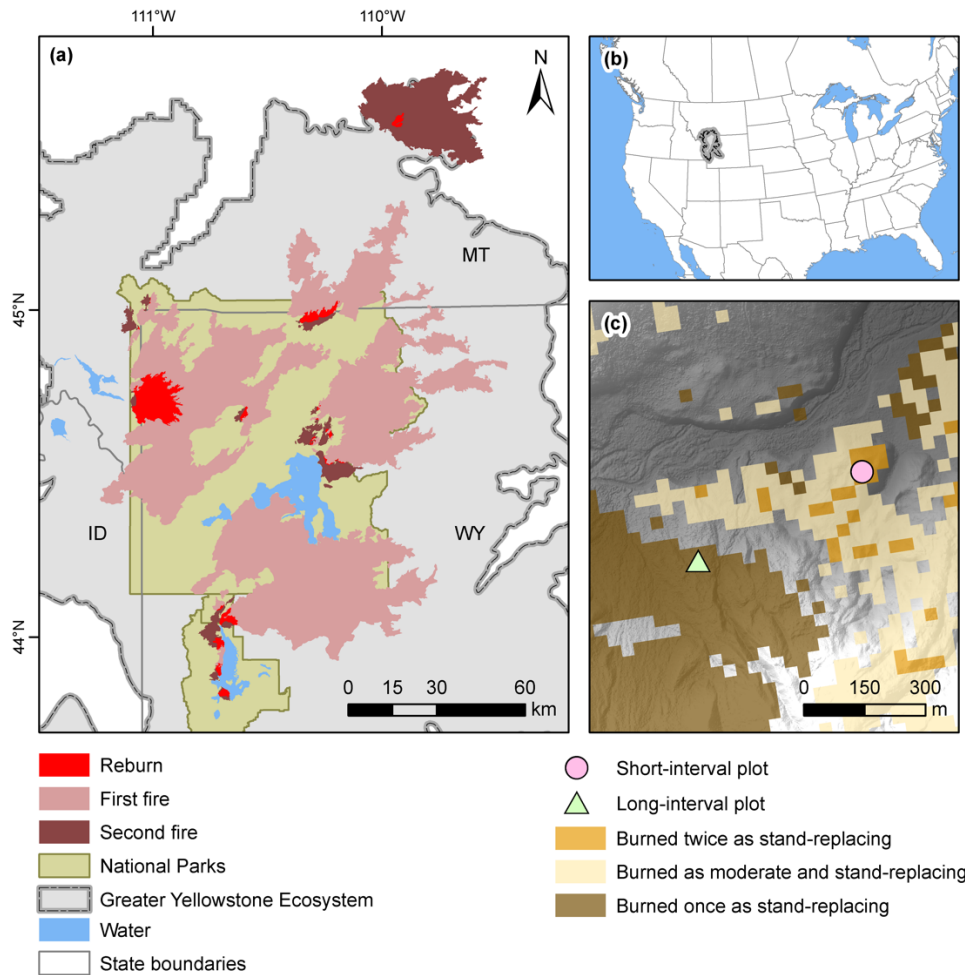


Figure 1. (a) Reburns sampled in 2021 in the GYE. Different shades show perimeter of first fires, second fires (long-interval), and reburned areas (short-interval). (b) Location of GYE within United States. (c) Paired plot site in the 2016 Berry Fire reburn of the 2000 Wilcox Fire, Grand Teton National Park. Short-interval plots burned twice as stand-replacing fire and long-interval plots only burned as stand-replacing in the most recent fire. Shading shows underlying topography.

Subalpine forests cover much of the GYE between ~1900-3000 m elevation and historically recovered rapidly after infrequent severe fire due to prevalent serotinous lodgepole pine with its fire-stimulated canopy seed bank (Turner et al. 1999). Stand-level percent serotiny of lodgepole pine is highest at lower elevations (up to ~2300-2400 m; Tinker et al. 1994, Schoennagel et al. 2003). Other tree species in the subalpine zone include Douglas-fir (*Pseudotsuga menziesii* var. *glauca*) and quaking aspen (*Populus tremuloides*) at lower elevations, Engelmann spruce (*Picea engelmannii*) and subalpine fir (*Abies lasiocarpa*) at higher elevations, and whitebark pine (*Pinus albicaulis*) near upper treeline (Baker 2009). Douglas-fir, Engelmann spruce, subalpine fir, and non-serotinous lodgepole pine rely on wind dispersal from nearby live seed sources, and most seeds fall within 50 m of a live tree (McCaughay and Schmidt 1987, Gill et al. 2021). Whitebark pine and quaking aspen can disperse over longer distances (Turner et al. 2003, Lorenz et al. 2011), and aspen can also resprout after fire (Baker 2009).

Reburn and plot selection

We selected recent (1994-2018) fires that severely burned subalpine forests at both short (< 30-year; $n = 16$ "reburns") and long (> 125-year) intervals (Figure 1a; Eidenshink et al. 2007). We sampled 1-2 plot pairs per reburn that each consisted of a 0.25-ha short-interval plot burned twice as stand-replacing fire and a topographically similar, nearby 0.25-ha long-interval plot burned as stand-replacing in the same recent fire (Figure 1c). These data were augmented with previously collected paired plot data from 12 years after the 1988 fires (Schoennagel et al. 2003). Together, these datasets included 33 plot pairs ($n = 66$ plots) widely distributed throughout the GYE and representing a range of short fire return intervals, time since most recent fire, and topographic conditions (Figures 1a, 2).

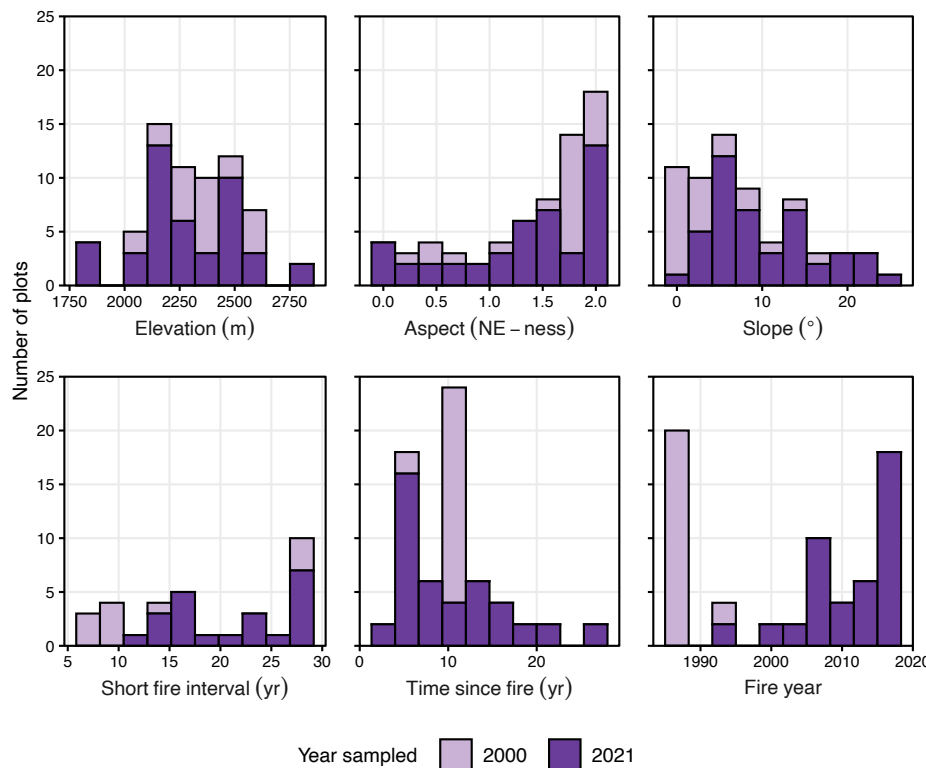


Figure 2. Histograms showing general characteristics of plots sampled in 2021 ($n = 44$, this study) and 2000 ($n = 22$) including elevation, aspect where 0 is southwest and 2 is northeast, slope, short fire interval, time since most recent fire, and year of most recent fire. Short fire interval is only summarized for short-interval plots.

Field data collection

Forest recovery and fuels were sampled in 0.25-ha plots following standard methods (Nelson et al. 2016, Turner et al. 2019). Sapling/seedling, tree, and standing dead stem density were tallied in three parallel 2-m x 50-m belt transects. At 5-m intervals, we measured height, crown base height for live stems, and diameter at breast height (DBH) of the closest live tree by species and standing dead snag; height of the closest sapling/seedling by species; and cover and average height of shrubs by species in 0.25-m² quadrats ($n = 25$ quadrats for 6.25-m² per plot). Downed woody and forest floor fuels were quantified with five 20-m Brown's planar intersect transects (Brown 1974) oriented randomly from plot center (total length = 100 m per plot). We recorded 1-h (< 0.64 cm diameter) and 10-h (0.64-2.54 cm) fuels along the first 3 m, 100-h (2.54-7.60 cm) fuels along the first 10 m, and sound and rotten coarse woody debris (> 7.6 cm diameter, 1000-h fuel) along the full 20 m. Litter and duff depth were recorded at 2-m intervals at three locations per transect ($n = 15$ measurements per plot). At plot center we measured aspect, slope, and distance to unburned live forest edge. If live edge was not visible or too far to measure in the field, this distance was estimated in ArcGIS Desktop 10.6 from aerial imagery and burn severity perimeters. Field data from 2000 included stem densities by species counted in four parallel 2-m x 50-m belt transects spaced 25 m apart (Schoennagel et al. 2003).

Biomass and fuels calculations

We derived live tree, dead snag, lodgepole pine sapling, and shrub aboveground biomass using allometric equations (Cole 1971, Brown 1978, Gholz et al. 1979, Ker 1984, Harmon and Sexton 1996, Means et al. 1996, Ter-Mikaelian and Korzukhin 1997, Turner et al. 2004). Snag biomass was summarized by size classes corresponding to downed wood (i.e., 1-, 10-, 100-, and 1000-h based on DBH). Canopy fuel load and bulk density were estimated from conifer tree crown biomass. Dead woody fuel biomass was computed for 1-, 10-, 100-, and 1000-h pools following Brown (1974) and correcting for slope. Litter and duff biomass were quantified based on average depth and bulk densities for lodgepole pine forest types (Brown et al. 1982; Nelson et al. 2016).

Question 1: Effects of short-interval fire, climate, and other factors on forest recovery

We tested whether live tree stem densities were lower in short- versus long-interval fire with a one-sided, paired Wilcoxon signed rank test ($n = 33$ pairs, lower densities expected in reburns). Differences were also evaluated by species. For lodgepole pine, which was present in all plots, a two-sided, paired Wilcoxon signed rank test was used. For other species, which were absent from many plots and exhibited high variance relative to mean values, differences in presence and density between pairs were tested with zero-inflated negative binomial regression models adjusted for matched data (McElduff et al. 2010, Abadie and Spiess 2022). Subsequent analyses only used live conifer stem densities (i.e., excluding aspen).

Post-fire climate was characterized with water-year (October-September) climate water deficit and summer (June-August) vapor pressure deficit (VPD; Harvey et al. 2016b; Stevens-Rumann et al. 2018; Davis et al. 2019). We used 4-km resolution climate data (TerraClimate; Abatzoglou et al. 2019) and summarized 30-year normal (1989-2018) and 3-year post-fire anomaly (z-score relative to normal). We assessed whether warmer-drier climate amplified differences in conifer stem density using Spearman's rank correlations because pairwise bivariate distributions were not normal.

The relative importance of drivers of post-fire stem density was tested with multiple linear regression models ($n = 66$ observations). Predictors included climate (climate water deficit normal and post-fire summer VPD anomaly), short-versus long-interval fire, lower (< 2350) versus higher elevation as a proxy for stand-level serotiny, topography (heat load index and topographic position index), and distance to unburned edge. Continuous predictors were not strongly correlated (Pearson's $|r| < 0.5$) and were rescaled to have a mean of 0 and standard deviation of 1. Conifer stem density was log10-transformed to meet assumptions of linearity, normality, and equal variance, which were assessed with residual and quantile-quantile plots. We fit a full model including interactions between each predictor and short- versus long-interval fire. We used exhaustive model selection to identify the most important factors based on model Bayesian Information Criterion (BIC), retaining all models with difference in BIC < 2.

Question 2: Forest biomass and fuels after short- versus long-interval fire

We assessed whether total live and dead tree biomass were lower in short- versus long-interval fire with one-sided, paired t-tests ($n = 22$ pairs for live and $n = 21$ for dead fuels, lower biomass expected following reburns) and tested whether differences were amplified at sites with drier normal climate water deficit using Spearman's rank correlations. Individual fuel pool differences were tested using either two-sided, paired t-tests or two-sided, paired Wilcoxon signed rank tests. Fuels were transformed as needed to meet normality based on quantile-quantile plots, and a Wilcoxon test was used if transformations did not result in normal distributions. Trees, canopy fuels, and very small snags were absent from > 40% of plots and were not tested for differences. Finally, fuel pools were averaged over 0-10, 10-20, and 20-30 years since fire to explore trajectories of biomass change and recovery following short- versus long-interval fire.

Question 3: Comparing UAS data collection methods and derived forest measurements

In a subset of three 15-year-post-fire plots that burned in the 2006 Derby Fire and ranged from low to high post-fire tree density, overlapping imagery was acquired using a DJI Phantom 4 Pro V2.0. Eight GCPs were placed within or immediately outside the plot (Figure 3). One GCP was located at or near plot center, four at or near the midpoint on each side of the plot, and three distributed within the plot; starting from these locations, we placed GCPs in areas that were relatively flat and with minimal overhead vegetation that would obstruct the view from above. GCP locations were recorded with using an EMLID Reach RS2 base station and rover Global Positioning System (GPS) setup. Relative to the base station, GCP vertical accuracy averaged 0.011 m root-mean-square error (RMSE) and horizontal accuracy averaged 0.014 m RMSE. The UAS was equipped with two sensors, a conventional built-in sensor measuring red, green, and blue wavelengths (~660/550/470 nm, respectively; Fernandez-Figueroa et al. 2022; 20 megapixel resolution; hereafter

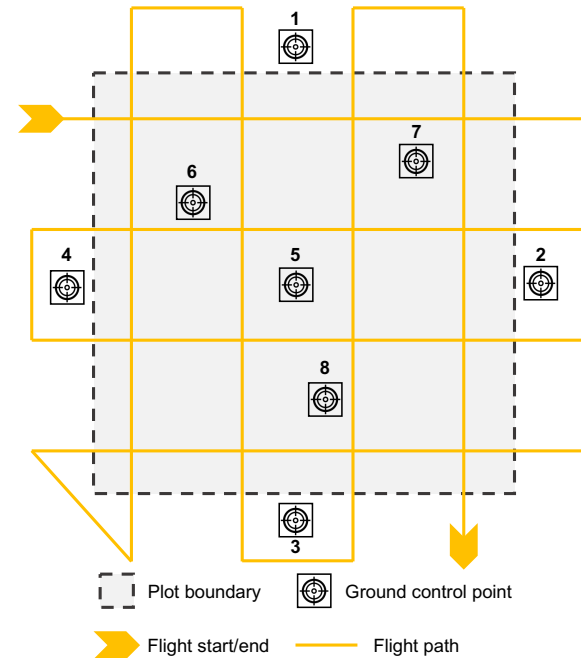


Figure 3. Plot and mission layout for UAS data collection.

"RGB") and a MAPIR Survey 3W sensor that measured red, green, and near-infrared wavelengths (660/550/850 nm, respectively; 12 megapixel resolution; hereafter "RGN"). Missions were flown within 1.5 hours of solar noon and planned using Map Pilot Pro software at 40 m above ground level, although flying altitude varied due to underlying topography. Each plot was flown twice in a grid pattern (Figure 3), once with sensors directed straight down (nadir) and the second with sensors directed at an angle (oblique, 15° RGB, 10° RGN). Raw imagery (i.e., RAW format) was collected with 75% lateral overlap and either 75% forward overlap (RGB) or approximately 90% forward overlap (RGN). A photo of a MAPIR reflectance calibration target was taken immediately before each flight.

We performed DAP processing for different potential scenarios for ground control points (0, 1, 5, or 8) and sensor angles (nadir only or nadir plus oblique) for RGN imagery only, because we expected collecting near infrared reflectance would improve tree versus snag detection relative to RGB imagery. Prior to DAP processing, radiometric calibration was performed for RGN images using MAPIR software and the corresponding calibration reflectance target photo. RGB and RGN imagery were separately processed using Agisoft Metashape Professional 1.6.2 to create classified 3D point clouds, orthorectified image mosaics, and digital elevation models (DEMs) for each plot. Processing parameters included: ultra high accuracy (50,000 keypoints, 10,000 tiepoints), mild filtering, and point classification as belowground, ground, or aboveground (0.7 m cell size, 1.1° max angle, 1.0 m max distance, which were recommended as default values by local experts). The DEM was created from points classified as ground using Inverse Distance Weighting interpolation.

Forest structure estimation and snag classification was performed in R 4.1.3 (R Core Team 2022), primarily using the lidR package (Roussel et al. 2020). Point clouds were first filtered to remove duplicates and normalized to the DAP-derived DEM. Tree tops were located using points classified as aboveground (> 0.1 m height) and a 1 m diameter moving window to detect local maxima. Individual points were then assigned to a tree (i.e., tree segmentation; Dalponte and Coomes 2016). Trees > 1.4 m height were classified as either tree or snag using unsupervised k-means classification on the mean, max, and coefficient of variation of all three bands (RGB or RGN). Based on iterative trial runs, we used 10 clusters and classified snags as the cluster with the highest mean blue intensity for RGB or lowest mean near-infrared intensity for RGN. We classified all individual trees > 5 m height as snags given that young regenerating trees were shorter. Stems and snags were tallied by height class (live stems > 0.1 m height, trees > 1.4 m height, snags) and summarized by DAP-derived mean, 90th percentile, and max height. Total live aboveground biomass was estimated by summing individual whole tree biomass derived from allometric equations based on height (Brown 1978). Plot measurements derived from UAS DAP were compared to field measurements using 1:1 lines and normalized RMSE; differentiation between snags and trees was visually assessed based on point clouds; and sampling effort, cost, post-processing time, and point cloud and DEM error and resolution were evaluated for different data collection methods.

All analyses and visualizations were performed in ArcGIS Desktop 10.6 and R. Code and data are publicly available on Github (https://github.com/kbrazuun/Braziunas_etal_SIL and <https://github.com/kbrazuun/PointCloudProcessing>).

Results and Discussion

Question 1: Effects of short-interval fire, climate, and other drivers on forest recovery

Live stem densities were an order of magnitude lower following short- compared to long-interval fire (mean 3,240 versus 28,741 stems ha^{-1} , median 2,000 versus 5,000 stems ha^{-1} , respectively; Figure 4). Tree species presence did not differ between plot pairs, but conifer densities were 68–92% lower following short-interval reburns (Figure 5, Table D1). In contrast, aspen density was over 500% higher in short-interval plots (Figure 5, Table D1).

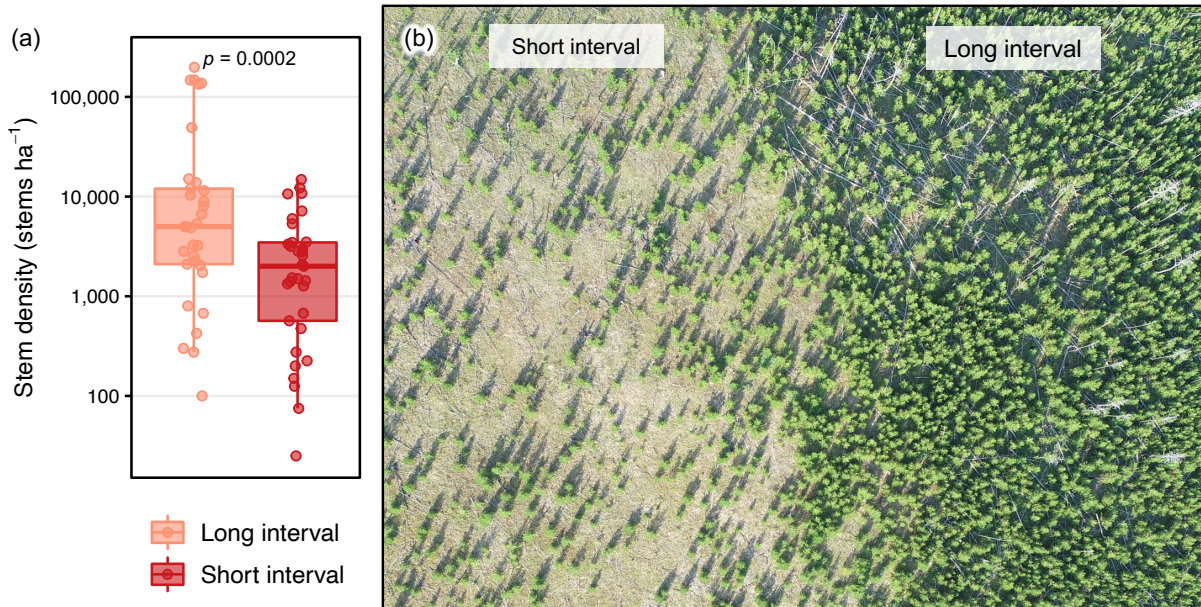


Figure 4. (a) Total live stem density boxplots for long- and short-interval plots. Points show raw data. Differences are significant at $p = 0.0002$ based on a one-sided, paired Wilcoxon signed rank test (test statistic $V = 478$, $n = 33$ pairs). (b) Aerial view of forest recovery and variation in fuels following the 2006 Derby Fire, which reburned the 1990 Iron Mountain Fire as short-interval fire (left) and burned older forest as long-interval fire (right). Photo credit: Kristin Braziunas

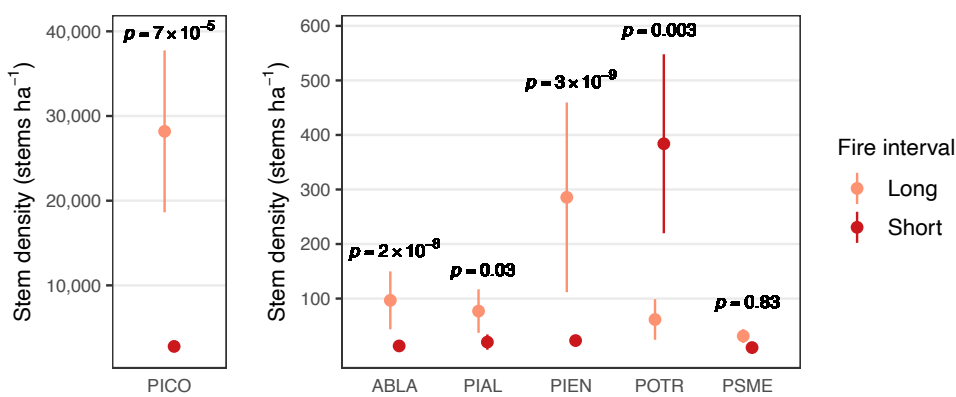


Figure 5. Stem density by species in long- versus short-interval plots ($n = 33$ pairs). Points are means \pm 1 standard error. Differences in lodgepole pine density were tested with a two-

sided, paired Wilcoxon signed rank test (test statistic = V). Differences in density for other species were tested with zero-inflated negative binomial regression models adjusted for matched data (test statistic = t , $df = n - 1$). ABLA: Subalpine fir, PIAL: Whitebark pine, PICO: Lodgepole pine, PIEN: Engelmann spruce, POTR: Quaking aspen, PSME: Douglas-fir.

Warmer-drier climate was associated with greater differences in conifer density between paired plots. Differences in long- minus short-interval stem density were strongly positively correlated with climate water deficit normal ($\rho = 0.67$, $p = 0.00002$, $n = 33$; Figure 6a) and weakly positively correlated with summer vapor pressure deficit anomaly ($\rho = 0.34$, $p = 0.05$, $n = 33$; Figure 6b).

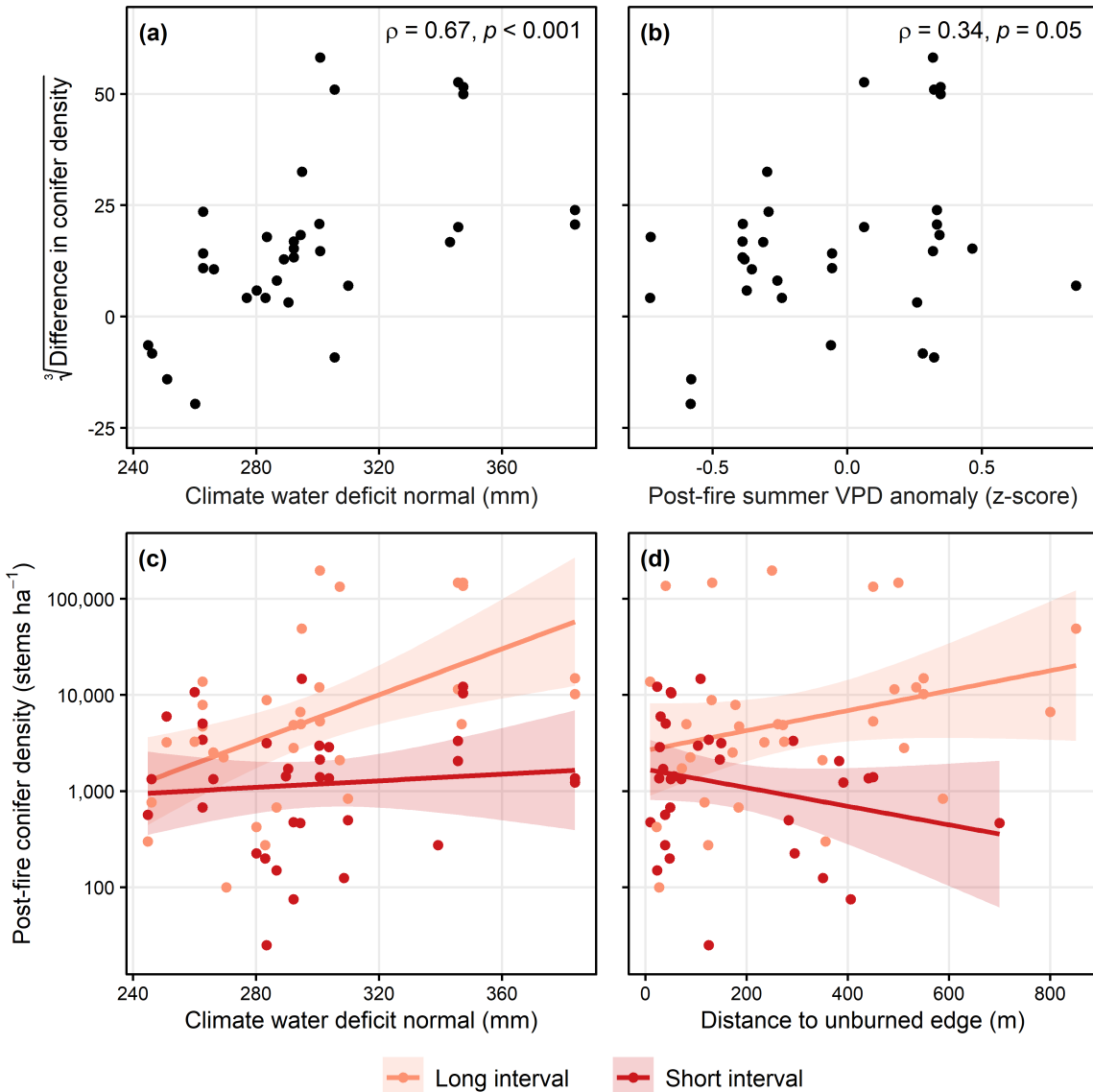


Figure 6. Pairwise relationships between (a) climate water deficit normal (1989–2019) or (b) 3-year post-fire summer vapor pressure deficit (VPD) anomaly and differences in live conifer stem density in long- minus short-interval paired plots ($n = 33$). Differences in conifer density have been cube-root transformed for plotting. Interactions between fire interval and (c) climate water deficit normal or (d) distance to unburned forest edge explained post-fire live conifer stem density ($n = 66$). Points and lines are colored by long- (light peach) or short-interval (dark red) fire. Y axis is on a log10 scale. Lines are linear fits and shading is standard error.

Higher post-fire stem densities were best explained by long fire return intervals, higher climate water deficit normal (i.e., warmer-drier conditions), and interactions of fire interval with both distance to unburned edge and deficit (Figure 6c,d; Table 1). Following short-interval fire, stem densities declined at farther distances from unburned edge and diverged from long-interval densities with warmer-drier climate. Models explained a relatively low amount of variation (adjusted $R^2 < 0.3$ for all models), and most variance was explained by the main effects of fire interval and climate water deficit (adjusted $R^2 = 0.23$ for model without interactions).

Table 1. Multiple linear regression models predicting stem density (log10-transformed) from multiple factors and potential interactions with short-interval fire.

Model	ΔBIC	Adj. R^2	Predictor	Estimate	SE	t	p
Model 1	0	0.28	(Intercept)	3.70	0.13	29.01	2×10^{-37}
			Fire interval (short)	-0.74	0.18	-4.03	0.0002
			Climate water deficit normal	0.28	0.09	3.02	0.004
			Distance to unburned:Fire interval (short)	-0.34	0.16	-2.19	0.03
			Distance to unburned:Fire interval (long)	0.12	0.12	0.96	0.34
Model 2	0.7	0.27	(Intercept)	3.74	0.12	30.60	4×10^{-39}
			Fire interval (short)	-0.67	0.17	-3.87	0.0003
			Climate water deficit normal	0.43	0.12	3.55	0.0008
			Climate water deficit normal:Fire interval (short)	-0.37	0.17	-2.12	0.04
Model 3	1.1	0.23	(Intercept)	3.74	0.13	29.77	8×10^{-39}
			Fire interval (short)	-0.67	0.18	-3.77	0.0004
			Climate water deficit normal	0.25	0.09	2.81	0.007
Model 4	1.7	0.29	(Intercept)	3.72	0.13	29.17	4×10^{-37}
			Fire interval (short)	-0.74	0.18	-4.01	0.0002
			Climate water deficit normal	0.40	0.13	3.09	0.003
			Distance to unburned:Fire interval (short)	-0.28	0.16	-1.72	0.09
			Climate water deficit normal:Fire interval (short)	-0.24	0.19	-1.30	0.20
			Distance to unburned:Fire interval (long)	0.07	0.12	0.59	0.56

Note: Continuous predictors were standardized to have a mean of 0 and standard deviation of 1.

Question 2: Forest biomass and fuels after short- versus long-interval fire

Short-interval plots had over seven times less aboveground live tree/shrub biomass and half as much dead woody biomass compared to long-interval plots (Figures 7, 8). Warmer-drier site conditions amplified differences in live ($\rho = 0.63$, $p = 0.002$, $n = 22$) but not dead biomass ($\rho = 0.14$, $p = 0.5$, $n = 21$; Figure 9). Differences in live biomass were reflected in tree biomass, available canopy fuel load, canopy bulk density, and lodgepole pine sapling biomass. Live shrub biomass was low and similar between plot pairs.

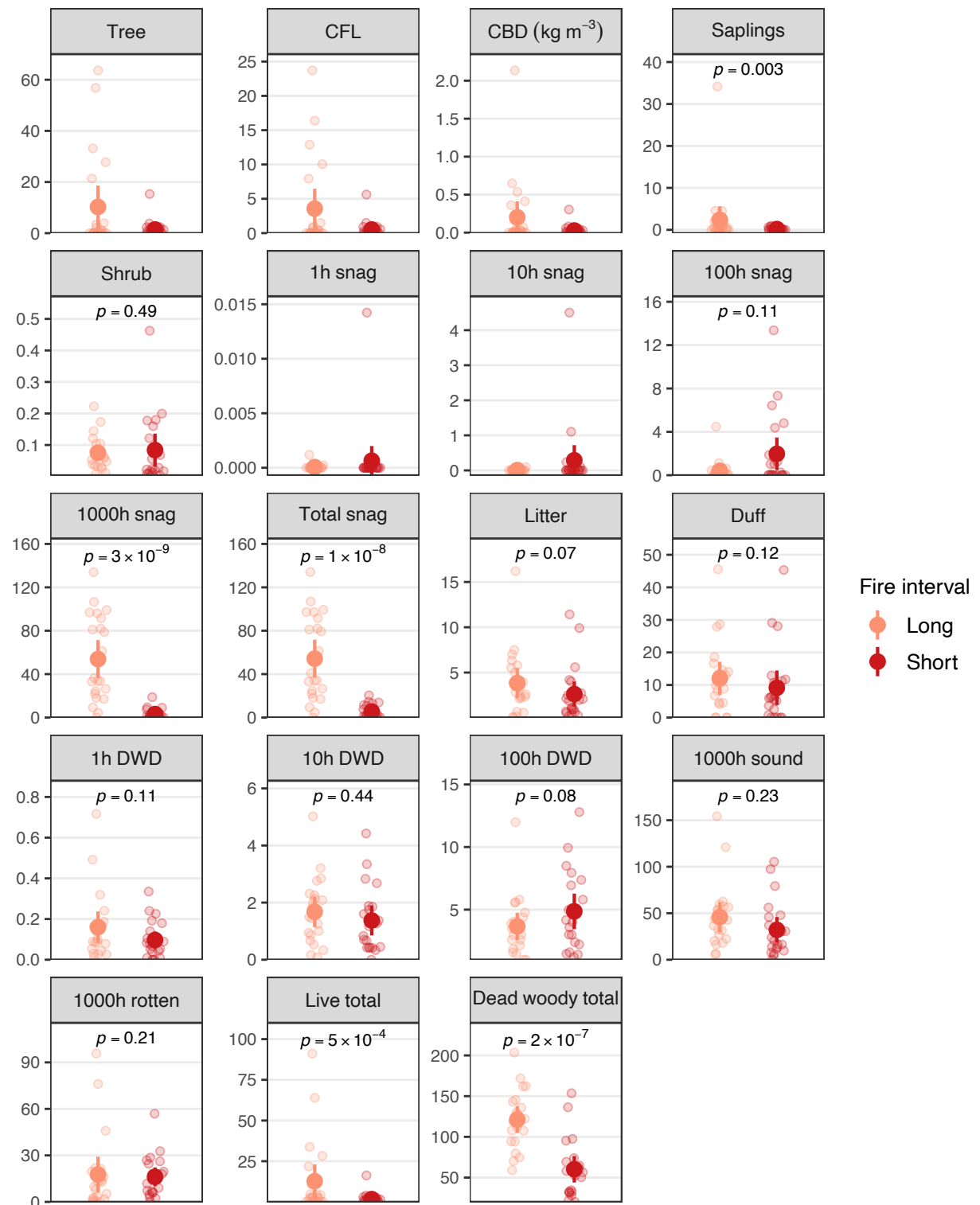
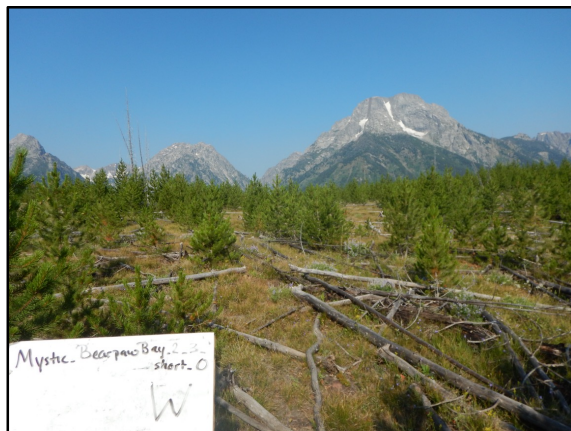


Figure 7. Biomass and fuels following long- versus short-interval fire. Solid points are mean values with 95% confidence intervals. Shaded points show all data. All values are in Mg ha^{-1} unless otherwise noted. All $n = 22$ except for shrubs ($n = 20$) and dead surface fuels ($n = 21$). Shown p-values are results of either Wilcoxon signed rank or paired t-test (see Table D2). CFL: Canopy fuel load, CBD: Canopy bulk density, DWD: Downed woody debris.

Compared to long-interval plots,

short-interval paired plots had...



...seven times less live tree/shrub biomass.



...half as much dead woody biomass.



...five times higher aspen density.

Figure 8. Illustrative photos of long- and short-interval plot pairs highlighting differences in live woody biomass and associated conifer regeneration density, dead woody biomass and fuels, and aspen regeneration density. Photo credit: Kristin Braziunas

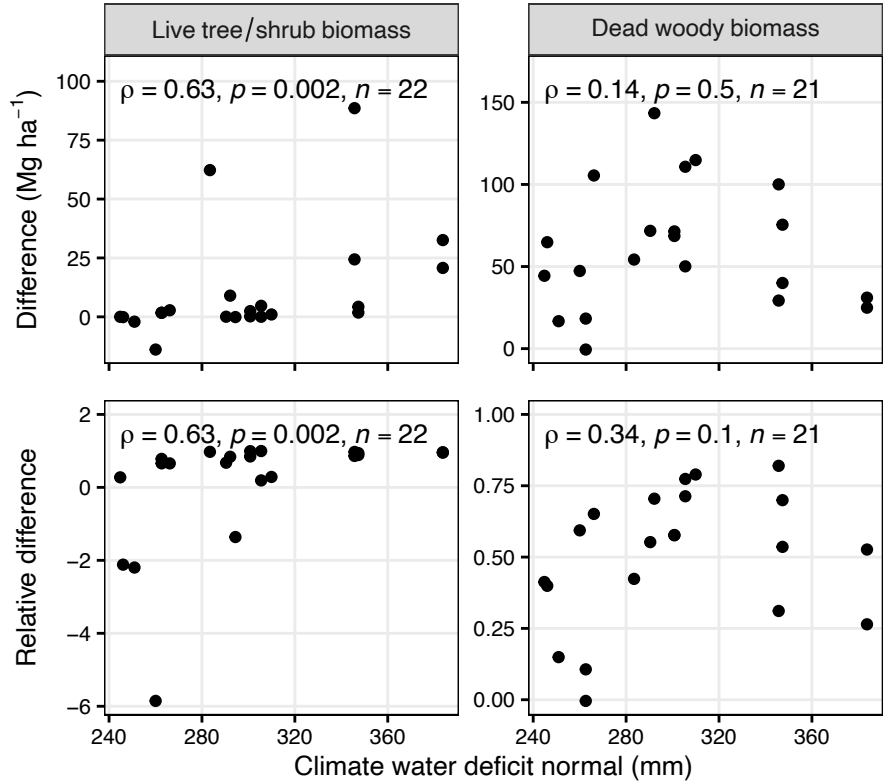


Figure 9. Pairwise relationships between climate water deficit normal (mm; 1989–2018) and actual and relative differences in paired long- and short-interval aboveground live tree/shrub ($n = 22$) and dead woody ($n = 21$) biomass. Plots show the strength of pairwise relationships (Spearman's rank correlation) and significance (p-value).

Individual snag and downed woody pools were highly variable and mostly did not differ between short- and long-interval plots (Figure 7). Large, 1000-h (> 7.6 cm diameter) snags were the primary driver of lower dead woody fuel loads in short-interval plots (Figures 4b, 7). Although the majority ($> 80\%$) of dead woody fuels were in 1000-h pools in all plots, the proportion of dead wood in 100-h fuels increased from 2 to 15% following short-interval reburns (Figure 10). Litter and duff loads did not differ between plot pairs.

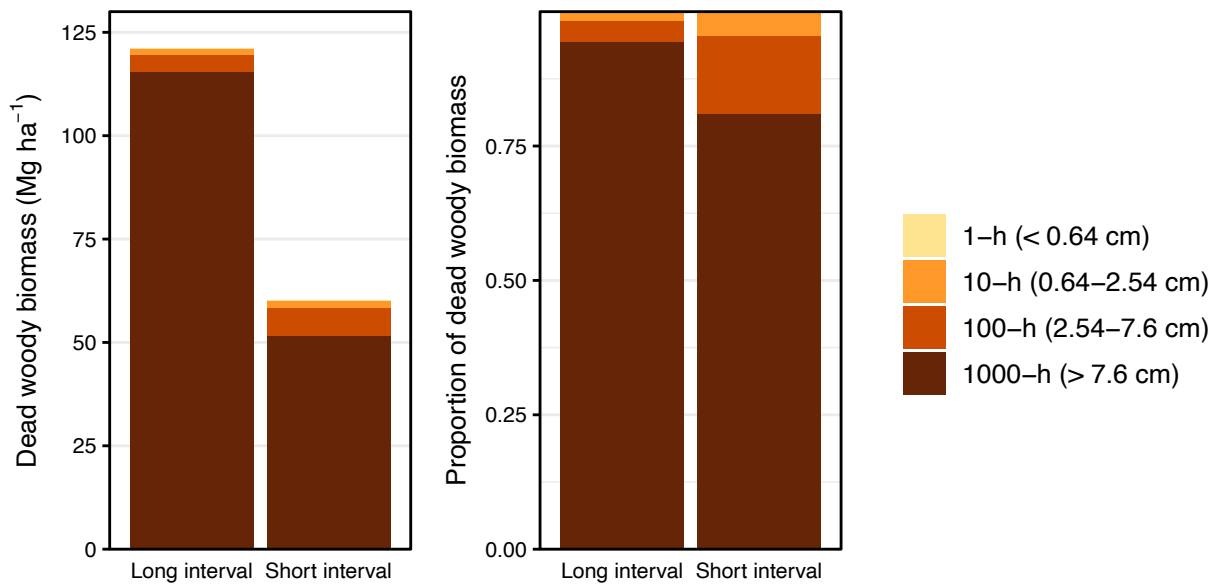


Figure 10. Biomass of dead woody fuels by size class, including standing dead snags and downed woody debris.

Total live plus dead biomass increased over time following long-interval fire and allocation shifted among standing dead, downed wood, and live pools; in contrast, total live plus dead biomass changed little during the first 30 years after short-interval fire (Figure 11). Live tree biomass accumulated more rapidly following long- compared to short-interval stand-replacing fire. Long-interval plots had much higher snag biomass immediately after fire, which increased accumulation of downed wood over time.

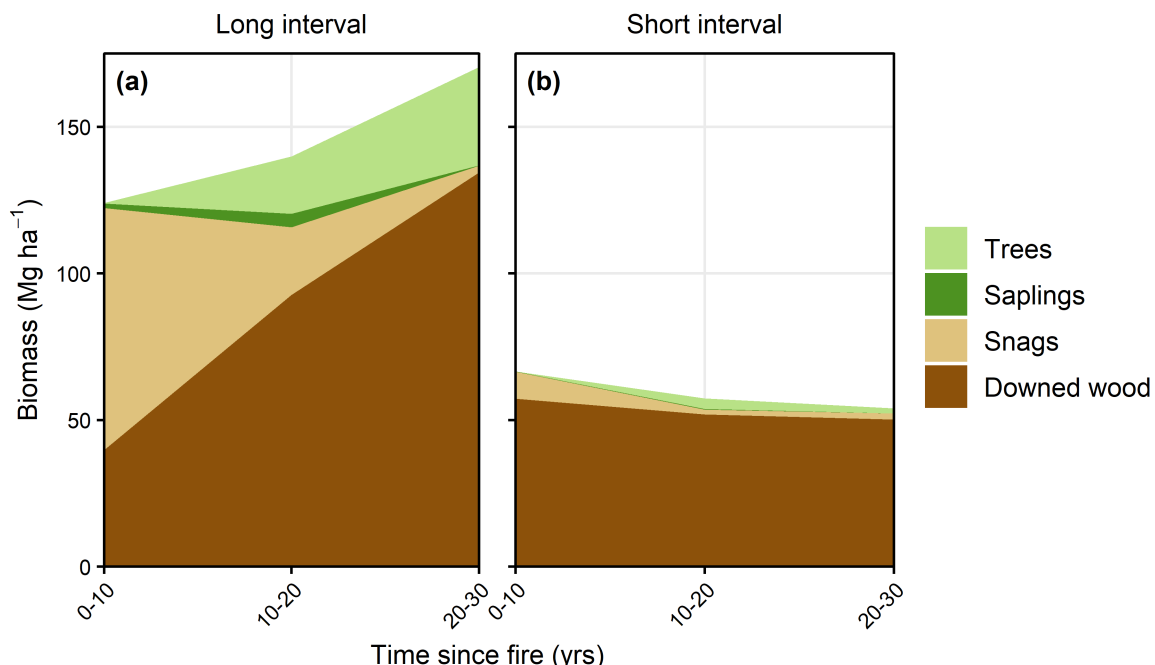


Figure 11. Aboveground live and dead biomass pool trajectories following (a) long- and (b) short-interval fire. Pools are averaged in 10-year bins (0-10, 10-20, and 20-30 years since fire).

Question 3: Comparing UAS data collection methods and derived forest measurements

All UAS data collection methods resulted in underprediction of stem, tree, and snag density, as well as total tree biomass in young, dense, post-fire stands (Figures 12, 13). DAP-derived data from RGB imagery accurately ranked plots in order from low to medium to high density and biomass for all stems, trees, and snags. In contrast, using RGN imagery did not consistently differentiate between medium- and high-density plots. Height was better estimated than density for both sensors, but only RGB imagery enabled the detection of the tops of tall snags (Figure 14). The use of GCPs and oblique sensor angles had minimal effect on all forest structure metrics derived from RGN imagery, and the highest quality RGN dataset (8 GCPs, nadir plus oblique imagery) did not consistently outperform other RGN datasets (Figures 12, 13).

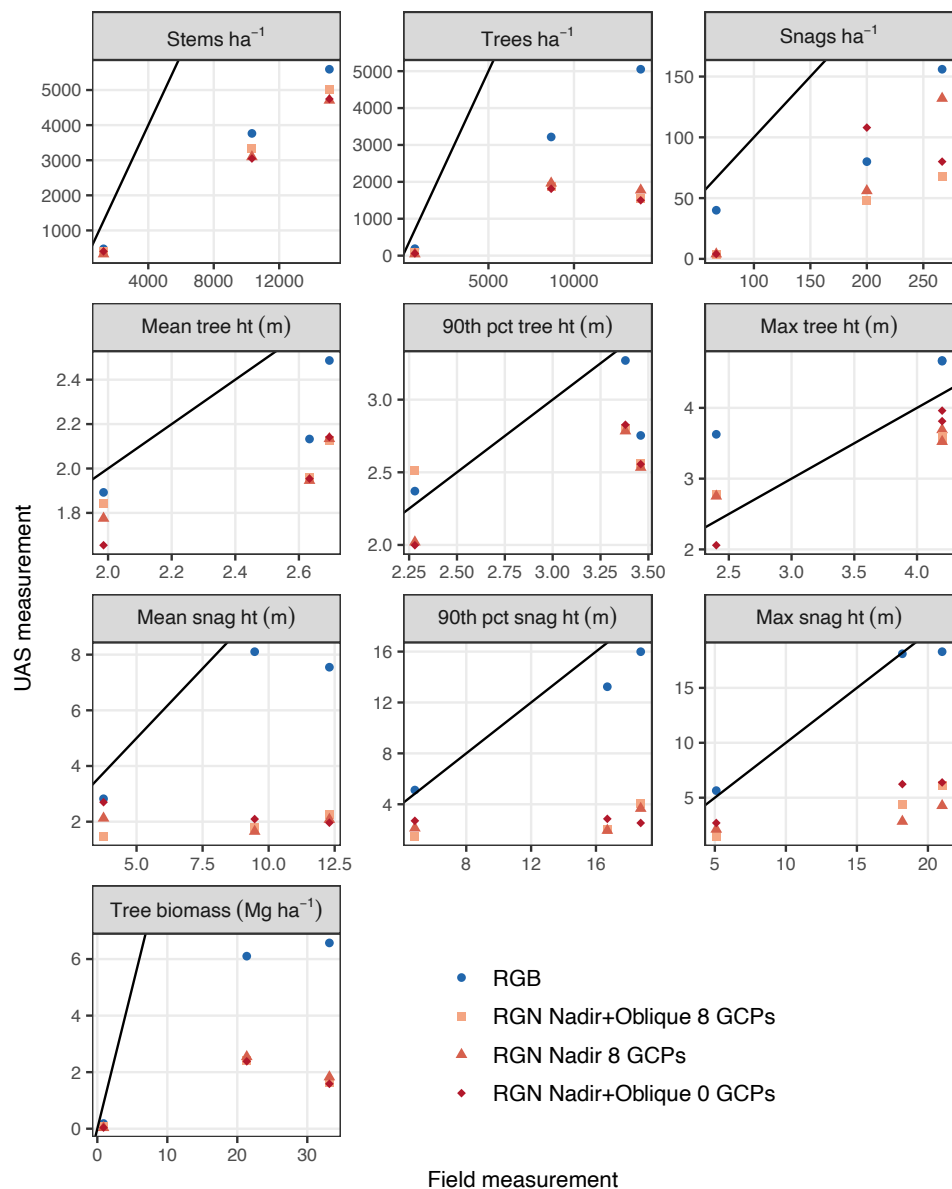


Figure 12. Comparison of UAS and field measurements for metrics of forest structure, relative to a 1:1 black line. Four data collection scenarios are shown. RGB: Red, green, and blue band sensor; RGN: Red, green, and near-infrared band sensor; GCP: Ground control point.

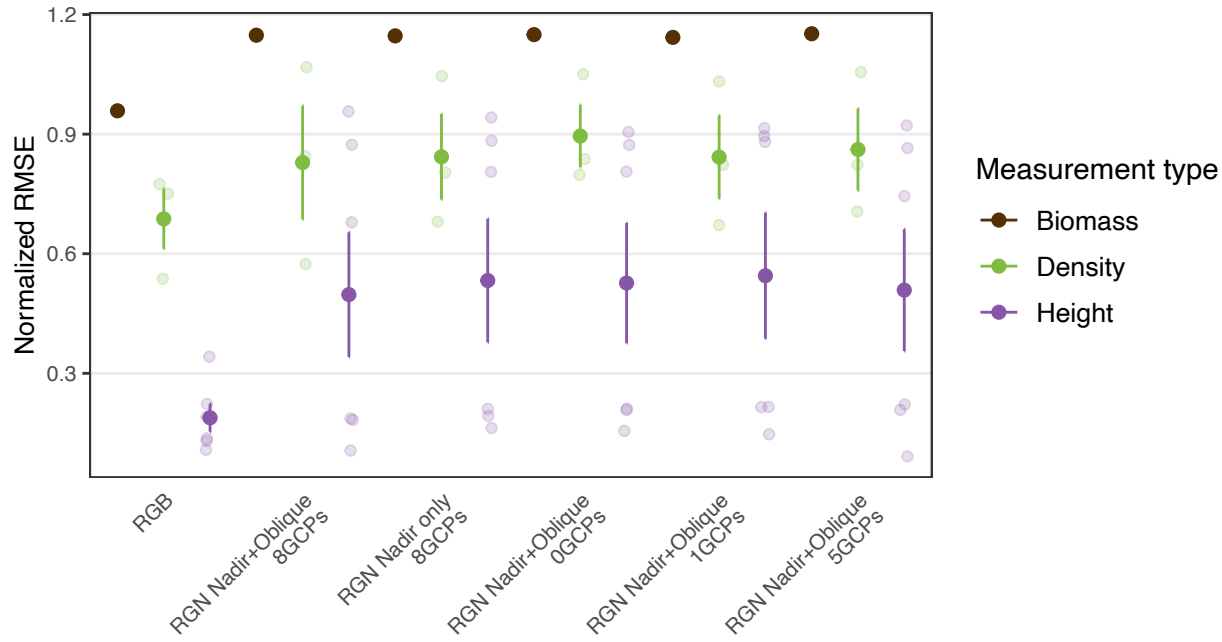


Figure 13. Normalized RMSE for UAS DAP-derived measurements of forest structure relative to field measurements. Normalized RMSE is RMSE divided by the mean observed value, which enables comparison across metrics with different units. Solid points are mean values ± 1 standard error for each measurement type, shaded points are all observations. RMSE: Root-mean-square error; RGB: Red, green, and blue band sensor; RGN: Red, green, and near-infrared band sensor; GCP: Ground control point.

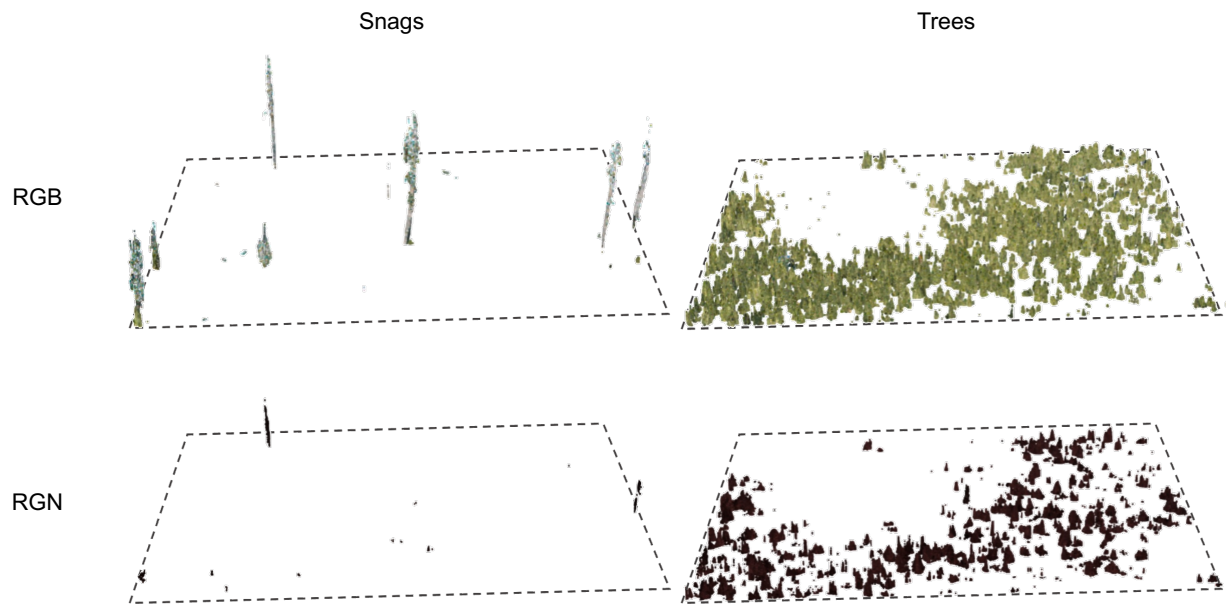


Figure 14. Point clouds for the medium density plot showing points classified as snags (left) and trees (right) using the RGB sensor (top) and RGN sensor (bottom). Both point clouds included nadir plus oblique images post-processed with 8 GCPs. Dashed lines show approximate plot boundary.

Sampling effort, cost, post-processing time, and point cloud and DEM error and resolution differed among UAS data collection methods (Table 2).

Sampling effort: Use of GCPs greatly increased sampling effort. Establishing GCPs in the field, recording GPS coordinates, and re-collecting GCPs following imagery acquisition was comparable to the time required to collect field data. This process usually required an extra visit to the plot and contributed to trampling and downed wood breakage within the plot, which can affect both DAP-derived and field measurements. Including oblique as well as nadir imagery required minimal additional effort (15-20 min for a flight, 1 extra battery), because the same plot setup and flight plan could be used with minor changes.

Cost: The additional cost of the RGN sensor with accessories (~\$700) plus GPS setup (~\$1900) was equivalent to the cost of the DJI drone plus extra batteries (~\$2500).

Post-processing time: Dense cloud processing takes the most computation time, so is used to compare approaches. Dense cloud processing of RGN imagery required substantially more time than RGB imagery (Table 2), most likely because there were approximately three times more images. Low density plots consistently took longer than higher density plots. Processing time can be reduced by filtering images or adjusting parameters, and processing is mostly automated. However, identifying GCP locations took 1-2 hours of hands-on time per plot, depending on the number of GCPs and images.

Point cloud and DEM error and resolution: Reprojection error, which measures the quality of image alignment, was consistently lowest while output resolution was consistently highest for the RGB compared to RGN sensor (Table 2). Point cloud density tended to be slightly higher when nadir plus oblique imagery was combined, although DEM resolution was similar. Using GCPs did not markedly alter error or resolution.

Table 2. Comparison among processing times, error, and spatial resolution after removal of duplicates for different methods of UAS data collection and plot tree density. Use of fewer GCPs had minimal effects on values presented in this table, so are not shown here.

Sensor (Mpix)	Angle	GCPs	Tree density	Dense cloud processing (hrs)	Reprojection error (pix)	Point density (pts cm ⁻²)	DEM resolution (cm)
RGB (20)	Nadir + Oblique	8	Low	19	0.55	0.58	1.58
			Medium	13	0.58	1.34	1.51
			High	8	0.41	1.40	1.65
RGN (12)	Nadir + Oblique	8	Low	77	3.37	0.28	2.55
			Medium	55	3.06	0.58	2.43
			High	42	2.81	0.53	2.69
RGN (12)	Nadir only	8	Low	30	3.32	0.26	2.51
			Medium	20	3.00	0.45	2.44
			High	15	2.87	0.43	2.66

Mpix: Megapixels; GCPs: Ground control points; RGB: Red, green, and blue wavelengths; RGN: Red, green, and near-infrared wavelengths

Discussion

Interacting drivers amplify effects on forest recovery. Independent effects of short-interval reburns, post-fire drought, and long distances to unburned forest on post-fire conifer densities are well documented (Stevens-Rumann and Morgan 2019), and here we found amplifying interactions. This is particularly concerning in western US forests, where current trends in climate, area burned, and stand-replacing fire indicate that these three conditions will co-occur with increasing likelihood (Harvey et al. 2016b, Westerling 2016, Buma et al. 2020). Interactions among drivers alter the likelihood of crossing recovery thresholds and the rate of ecosystem transformation (Scheffer and Carpenter 2003, Ratajczak et al. 2018). Our findings suggest that places where these drivers overlap could experience slower rates of forest recovery or be early hotspots for surprising forest change (Figure 15).

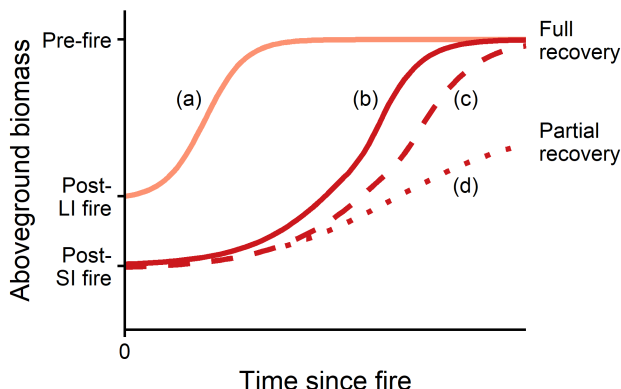


Figure 15. Potential recovery trajectories for aboveground biomass (live plus dead) after stand-replacing long- or short-interval fire. The starting point for each trajectory is the residual dead woody biomass after the fire. Following long-interval fire (a, light peach), biomass recovers rapidly to pre-fire levels. Following short-interval fire (b, solid dark red), biomass recovery is delayed and slower due to lower initial levels of dead biomass and tree regeneration. Average regeneration densities are sufficient that full biomass recovery is likely in the absence of subsequent disturbance. Amplifying effects of warmer-drier climate and/or long distances from seed source could further delay biomass recovery (c, dashed dark red) or potentially result in only partial biomass recovery if post-fire tree density is insufficient for self-replacement (d, dotted dark red). If stand-replacing fires reburn forests before they have recovered to pre-fire conditions, forests may be vulnerable to sustained reductions in biomass. LI: Long-interval; SI: Short-interval.

Aspen, on the other hand, emerged as a potential winner in a more fiery future. Quaking aspen effectively colonizes recently burned areas from seed via long-distance dispersal (Turner et al. 2003). Our results indicate that once underground root structures are established aspen resprout successfully and in abundance after short-interval reburns. Aspen is a keystone species of global importance for biodiversity (Rogers et al. 2020), and warmer climate is associated with inhibited growth and dieback of quaking aspen in the Rocky Mountains (Hanna and Kulakowski 2012). Our results highlight a potentially positive effect of climate-driven increases in short-interval fire, which by stimulating aspen regeneration may enable aspen expansion in favorable areas. Similarly, severe fire has catalyzed transitions from conifer to deciduous dominance in boreal forests (Johnstone et al. 2010; Mack et al. 2021).

Contrary to our expectations, warmer-drier site conditions were generally associated with higher conifer seedling densities, despite amplifying differences between short- and long-interval plots. This in part reflects the higher prevalence of lodgepole pine serotiny (Tinker et al. 1994) and longer growing seasons at lower elevations, which tend to be warmer and drier. An abundant serotinous seed bank may buffer forest recovery against shorter fire intervals. However, our results show that short-interval fire alters the strength of the relationship with average site climate, and Stevens-Rumann et al. (2018) found that 30-year climate water deficit switched from being associated with higher to lower likelihood of post-fire forest replacement under future conditions. In warm-dry subalpine sites, the negative effects of future drying on seedling establishment are likely to outweigh the positive effects of warming (Hansen and Turner 2019).

Reburns alter fuel recovery trajectories and potential future burn severity. Delayed recovery of live canopy fuels following short-interval stand-replacing fire suggests a lower likelihood of crown fire for 30 years or more following reburns. Average canopy bulk density in long-interval plots was already above an active crown fire threshold of 0.10 kg m^{-3} (Cruz et al. 2005), whereas average short-interval bulk density was well below. Self-regulating effects of past fires on future fire spread and burn severity are often short-lived (Parks et al. 2015, Buma et al. 2020), especially in subalpine forests (Harvey et al. 2016b), but our data show that regulation of canopy burn severity could be lengthened following short-interval fires.

Surface fire spread relies on fine surface fuels, which did not differ between plot pairs, suggesting future surface fire spread may be unaffected by reburns. Although we did not quantify herbaceous fuels, Schoennagel et al. (2004) found that herb and grass cover did not differ 12 years after short- versus long-interval fire in this region. Coarse woody debris does not contribute substantially to fire spread rates, but higher loadings can increase residence time, burn severity, and resistance to fire control (Graham et al. 2004, Sikkink and Keane 2012). Downed coarse wood loads of $22\text{-}67 \text{ Mg ha}^{-1}$ balance ecological benefits with fire hazard in cool-climate, post-fire forests (Brown et al. 2003). Average loadings following short-interval fire were within this range, but average long-interval loadings including large snags were much higher. Thus, short-interval reburns may reduce future surface burn severity even if they do not limit spread.

Implications for forest resilience and change. Overall, our results suggest that some characteristics of forest resilience remain intact after short-interval fire, while others are diminished or lost. All plots had tree seedlings and average densities in reburned areas were sufficient for self-replacement (Kashian et al. 2005), indicating that forest regeneration could be considered resilient even after two severe fires within a few decades (Figure 15). In terms of material disturbance legacies, downed coarse wood, which provides regeneration microsites, energy, nutrients, and carbon in post-fire environments (Harmon et al. 1986, Franklin et al. 2007), remained high following short-interval fires. In contrast, large standing snags, which serve as critical wildlife habitat for several bird species (Hutto 1995), were virtually absent in reburns. Total live and dead biomass was also much lower in reburns, and biomass accumulation was dampened relative to long-interval fire. These results suggest that short-interval fires weaken forest contributions to climate regulation via carbon sequestration. These diminished capabilities could be long-lasting and further amplified if stands reburn again within a few decades (Figure 15; Turner et al. 2019; Hayes and Buma 2021). However, negative feedbacks on burn severity from reduced fuel loads could still mitigate future fire effects and transitions to deciduous

species could enhance carbon uptake (Mack et al. 2021). Results of this study underscore the importance of considering amplifying interactions among drivers, the need for quantifying recovery over time scales long enough to detect trends, and the power of paired design to improve causal inferences from observational data. Interactions among multiple drivers diminished and delayed forest recovery and could lead to rapid, surprising changes in forest resilience during the 21st century.

Low-cost UAS shows promise and limitations for measuring young, dense conifer forests. Our results support the use of a low-cost UAS "out-of-the-box" for measuring some aspects of forest structure. Following standard approaches and without the use of training data, DAP processing of imagery collected with the built-in, 20 megapixel RGB sensor produced high-resolution point clouds, DEMs, and orthomosaics across a range of plot densities; captured relative differences in plot density; differentiated between snags and trees based on a combination of spectral information and height; and estimated reasonable stem heights. Our results also indicated that the labor-intensive deployment and post-processing of GCPs was not justified in this context. The most likely reason for the poorer performance of the RGN sensor was its lower spatial resolution (i.e., 12 megapixels). Even though the RGB sensor did not have a near infrared band, analyses using this imagery effectively differentiated live versus dead stems in young, post-fire plots. High-cost, cutting-edge technology or novel methods may be necessary for specific research applications (e.g., precision agriculture planning; Hunt and Daughtry 2018). However, we propose that for forest inventory and management, lower-cost and -capability systems may provide the necessary level of detail. Priority should be placed instead of identifying efficient data collection and processing approaches that can be consistently applied by different UAS pilots across multiple geographic regions.

Our methods of deriving post-fire forest structure from UAS data highlighted limitations and opportunities for improvement. Estimating tree density in young, post-fire, lodgepole pine dominated plots is particularly challenging, because plots often consist of small, densely packed trees with overlapping crowns. In our study, estimated biomass was the sum of individual trees and therefore errors in density estimation were propagated as errors in biomass estimation; for young forests where accurately estimating density is more error prone, a different approach should be used to derive tree biomass. A high-resolution, lidar-derived DEM could improve height estimates, especially when tree density is high, because lidar can penetrate the forest canopy (Wallace et al. 2016). Combining a single lidar flight with repeated imagery flights is recommended for creating a baseline forest inventory that can be regularly updated at low additional cost (Goodbody et al. 2019).

Science Delivery

The findings of this study were presented as part of a PhD Exit Seminar, "Operationalizing resilience of social-ecological systems to changing climate and fire in US Northern Rocky Mountain forests" in December 2021, which was a hybrid in person and online seminar, enabling broad participation. This work was also presented in a virtual Ecology and Evolutionary Biology Seminar at Kansas State University, "Anticipating future forests: Resilience, risk, and ecosystem services under changing climate and fire" (March 2022). A more general discussion of how forest and fire ecologists conduct research, including questions asked as part of this study, was included in two presentations to members of Madison, Wisconsin

Chapters of the P.E.O., which awarded a fellowship that partially supported Kristin Braziunas and this work (presentation title: “Sources of ignition: Becoming a fire ecologist”, March-April 2021), and in a profile of Kristin Braziunas in *Vital Signs 2020*, a publication by Grand Teton National Park. Results of this study informed portions of a field tour led by Monica Turner in July 2022 for the Superintendent of Grand Teton National Park and his leadership team. Findings will further be presented in a webinar on reburns hosted by the Northern Rockies Fire Science Network in March 2023 with co-presenter Tyler Hoecker (Climate Adaptation Postdoctoral Fellow, Northwest Climate Adaptation Science Center, University of Washington), who will present his work on short-interval fires and forest recovery in Glacier National Park.

A peer-reviewed journal article funded by this project (Braziunas et al., "Less fuel for the next fire? Warmer-drier climate amplifies effects of short-interval fire on forest recovery") is currently under review in *Ecology*. Data will be deposited at the Environmental Data Initiative upon acceptance for publication. A second journal article presenting post-fire understory plant communities following short- versus long-interval fire ("Peeking under the canopy: effects of short fire-return intervals on herbaceous understories of Greater Yellowstone," lead author Nathan G. Kiel) is in preparation; data were collected during the same field season in the same paired plots. N. G. Kiel presented this work at both the University of Wisconsin-Madison Center for Ecology and the Environment's Spring Symposium and the Biennial Scientific Conference on the Greater Yellowstone Ecosystem in May 2023. This work also informed N. G. Kiel's presentation to the Teton Chapter of the Wyoming Native Plants Society titled, "Peeking under the canopy: climate, fire, and Greater Yellowstone plant communities."

Given disruptions to field work, project timeline, and conference activity due to COVID, some deliverables have changed from the original proposal. K. H. Braziunas prioritized presenting results to targeted audiences in multiple virtual presentations rather than at a virtual conference or via a YouTube video. Drone imagery will be used in planned print and video products aimed at communicating to general audiences the potential magnitude of climate-driven landscape changes in Greater Yellowstone (Turner et al., in preparation). In addition, excellent best practice guides already exist for UAS data collection and processing; these are referenced in Github documentation. Code and data analysis associated with this project are publicly available via Github (https://github.com/kbrazuin/Braziunas_etal_SILI and <https://github.com/kbrazuin/PointCloudProcessing>).

Conclusions

Key Findings

Our study revealed that declines in subalpine forest recovery were amplified by interactions between climate and fire. Mean post-fire stem density was an order of magnitude lower following short- versus long-interval fires, and differences increased with greater annual climate water deficit. Because this amplification was most pronounced in landscape positions with a generally warmer-drier climate (i.e., 30-year normal), and only weakly related to anomalously warm-dry weather during the early post-fire years, our results suggest greater vulnerability to change at sites where moisture thresholds are already close. Furthermore, conifer regeneration in areas with historically robust serotinous seed banks is increasingly reliant on ex situ seed sources after short-interval fire and vulnerable to propagule limitation when far from unburned forest edges. Together, our findings suggest a trifecta of large stand-replacing patches

of short-interval fire in areas of higher moisture stress could threaten subalpine forest resilience. Differences in post-fire biomass between short- and long-interval plots highlight nuanced feedbacks between developing fuels and subsequent fire. Although many short-interval reburns had abundant downed wood, they had minimal additional input from snags and a higher proportion of fuels in smaller size classes that could decompose quickly or burn readily if fire recurs. In contrast to rapid recovery after long-interval fire, live biomass and canopy fuels remained low nearly 30 years after short-interval fire, suggesting prolonged self-regulation of future burn severity and delayed recovery of pre-fire biomass.

Using low-cost UAS, built-in sensors, and standard data processing and analysis methods can effectively characterize some aspects of young, post-fire forest structure such as height. However, for estimating density and biomass, additional steps and consideration are necessary. UAS output resolution and forest measurement accuracy were similar regardless of whether ground control points were used in data processing.

Management Implications

Forest structure and composition is expected to change substantially under future climate warming and fire activity. This will affect large areas of publicly owned and managed land, which provide a wide variety of public goods and ecosystem services such as timber, wildlife habitat, carbon storage, and scenic beauty. Forest managers will be on the front lines of navigating these changes. Our results suggest that areas where short fire interval, warm-dry climate position, and long distance to unburned forest edge overlap may be particularly vulnerable to reduced and slowed recovery of post-fire biomass. These could be high priority areas for replanting, if reforestation is desirable and likely to succeed, or areas where transitions to different forest conditions or to non-forest should be accepted, if future climate is likely to exceed tolerances of seedlings and trees. Some potential changes may be desirable in certain management contexts, such as increases in aspen density following short-interval fire.

Changing fuel loads after short-interval fire will likely affect fire behavior and effects, with implications for forest management and fire suppression. In areas such as Greater Yellowstone, forests historically recovered rapidly after long-interval fire and were able to burn again at high-severity after only a decade. Our results suggest that short-interval fire will delay biomass and fuels recovery in young, lodgepole pine-dominated forests, thus lengthening the time that post-reburn forests limit future fire intensity and spread. Considering the location and extent of reburned areas could be useful for anticipating fire behavior at landscape scales and planning fire suppression activities. In addition, reburns had lower loads of downed coarse wood relative to young forests recovering from long-interval fire. They may therefore provide better access or escape routes for firefighters.

Acquiring forest inventory measurements using UAS and DAP is well researched and understood, and this technology is primed for widespread use by forest managers. There are excellent resources already available documenting best practices, and established software and tools enable standardized data processing and analysis (see links on point cloud processing Github). UAS can be procured at low cost and learning to pilot a UAS requires some training and formal testing, but not highly specialized skills. One of the primary barriers we faced was flight restrictions; we were not allowed to fly over National Parks or any Department of Interior lands

due to policy restrictions at the time. It is important to identify and regulate the use of UAS, for example when they would interfere with air traffic, pose a threat to people or wildlife, or interfere with recreation or enjoyment of natural areas. However, we also suggest that aligning regulations to promote targeted use of UAS, especially by researchers and managers, could be desirable for generating large amounts of valuable forest data (Coops et al. 2019). Because UAS can be flown over areas that cannot easily be sampled (e.g., across a stream or river, or in steep topography where ravines or slopes make sites inaccessible), data derived from UAS can reduce personal safety risks to researchers.

Future Research

Our project suggests several opportunities for future research:

Fire behavior and post-fire fuels when forests reburn again. How will reburns affect future fire behavior, and how will fuel loads change if forests continue to burn more frequently? Our work suggests that reburns may reduce future fire intensity and severity, but not spread. These findings are consistent with the results of simulation modeling studies in the region (Braziunas et al. 2021, Turner et al. 2021). Future work should evaluate these expectations in areas that burn a third time at short, or even long, intervals. Changing fuel complexes, such as lower loads of large coarse woody logs but relatively higher proportions of small 100-h downed wood in reburns, could have nuanced effects on fire behavior and ecological impact.

Reburns, climate change, and recovery at regional to continental scales. How are interactions between changing climate and more frequent fire affecting forests across the western US? Effects of forest recovery and change after reburns have been highlighted in many recent studies (e.g., Whitman et al. 2019, Hayes and Buma 2021, Hoecker and Turner 2022). Syntheses of existing studies or broad-scale remote sensing studies should focus on similarities or differences among forest types and explore how interactions among multiple changing drivers (climate, fire frequency, seed availability) are likely to affect forests at continental scales.

The changing role of serotiny. How will prevalence and patterns of serotiny be affected by changes in fire activity? Stand-level percent serotiny of lodgepole pine in Greater Yellowstone varies with elevation and fire history (Tinker et al. 1994, Schoennagel et al. 2003). If fires occur more frequently and fires burn young stands before they have developed a serotinous seed bank, this may alter the relative share of serotinous and non-serotinous individuals in regenerating stands.

Robust evaluation of using oblique in addition to nadir imagery. How do images collected from multiple angles affect detection and measurement of trees and snags? Because our comparison between nadir-only and nadir plus oblique imagery was restricted to the RGN sensor, which did not detect standing dead snags well under either scenario, we propose that this is still an open research question. Including oblique sensor angles should provide additional data points to better characterize tall, small-diameter objects such as snags, and snag heights were well characterized by using RGB nadir plus oblique imagery. We suggest that future research should compare nadir-only, oblique-only, and different sensor angles to explore how this affects tree and snag detection and characterization. Depending on the total area flown, including multiple sensor angles (and multiple flights) in a mission may require minimal additional time

and effort, because many steps of mission planning do not need to be repeated.

Increased acquisition and assessment of UAS data for forest inventories. How well can forest structure, age, and composition be estimated using UAS-derived imagery across multiple forest types and conditions? Our project was limited to three plots in a similar forest type, stand age, and disturbance history. Estimates of forest structure derived from UAS DAP are more accurate when trees are large and widely spaced (Belmonte et al. 2020, Creasy et al. 2021). We recommend UAS be deployed across a wide range of forest conditions to assess how well actual and relative values are estimated. Priority should be placed on using low-cost systems with standardized approaches to data collection and processing that could enable data collection by many individuals across multiple management units and agencies, or by citizen scientists where appropriate.

Literature Cited

- Abadie, A., and J. Spiess. 2022. Robust post-matching inference. *Journal of the American Statistical Association* 117:983–995.
- Abatzoglou, J. T., D. S. Battisti, A. P. Williams, W. D. Hansen, B. J. Harvey, and C. A. Kolden. 2021. Projected increases in western US forest fire despite growing fuel constraints. *Communications Earth and Environment* 2:227.
- Abatzoglou, J. T., S. Z. Dobrowski, S. A. Parks, and K. C. Hegewisch. 2018. Terraclimate, a high-resolution global dataset of monthly climate and climatic water balance from 1958–2015. *Scientific Data* 5:170191.
- Baker, W. L. 2009. Fire ecology in Rocky Mountain landscapes. Island Press, Washington, DC.
- Belmonte, A., T. Sankey, J. A. Biederman, J. Bradford, S. J. Goetz, T. Kolb, and T. Woolley. 2020. UAV-derived estimates of forest structure to inform ponderosa pine forest restoration. *Remote Sensing in Ecology and Conservation* 6:181–197.
- Braziunas, K. H., D. C. Abendroth, and M. G. Turner. 2022. Young forests and fire: Using lidar-imagery fusion to explore fuels and burn severity in a subalpine forest reburn. *Ecosphere* 13:e4096.
- Braziunas, K. H., R. Seidl, W. Rammer, and M. G. Turner. 2021. Can we manage a future with more fire? Effectiveness of defensible space treatment depends on housing amount and configuration. *Landscape Ecology* 36:309–330.
- Brown, J. K. 1974. Handbook for inventorying downed woody material. USDA Forest Service, Intermountain Forest and Range Experiment Station, General Technical Report INT-16, Ogden, UT.
- Brown, J. K. 1978. Weight and density of crowns of Rocky Mountain conifers. USDA Forest Service, Intermountain Forest and Range Experiment Station, Research Paper INT-197, Ogden, UT.
- Brown, J. K., R. D. Oberheu, and C. M. Johnston. 1982. Handbook for inventorying surface fuels and biomass in the Interior West. USDA Forest Service, Intermountain Forest and Range Experiment Station, General Technical Report INT-129, Ogden, UT.
- Brown, J. K., E. D. Reinhardt, and K. A. Kramer. 2003. Coarse woody debris: Managing benefits and fire hazard in the recovering forest. USDA Forest Service, Rocky Mountain Research Station, General Technical Report RMRS-GTR-105, Ogden, UT.
- Buma, B., S. Weiss, K. Hayes, and M. Lucash. 2020. Wildland fire reburning trends across the US West suggest only short-term negative feedback and differing climatic effects.

- Environmental Research Letters 15:034026.
- Cole, D. M. 1971. A cubic-foot stand volume equation for lodgepole pine in Montana and Idaho. USDA Forest Service, Intermountain Forest and Range Experiment Station, Research Note INT-150, Ogden, UT.
- Coop, J. D., S. A. Parks, C. S. Stevens-Rumann, S. D. Crausbay, P. E. Higuera, M. D. Hurteau, A. Tepley, E. Whitman, T. Assal, B. M. Collins, K. T. Davis, S. Dobrowski, D. A. Falk, P. J. Fornwalt, P. Z. Fulé, B. J. Harvey, V. R. Kane, C. E. Littlefield, E. Q. Margolis, M. North, M. A. Parisien, S. Prichard, and K. C. Rodman. 2020. Wildfire-driven forest conversion in western North American landscapes. *BioScience* 70:659–673.
- Coops, N. C., T. R. H. Goodbody, and L. Cao. 2019. Four steps to extend drone use in research. *Nature* 572:433–435.
- Coops, N. C., P. Tompalski, T. R. H. Goodbody, A. Achim, and C. Mulverhill. 2022. Framework for near real-time forest inventory using multi source remote sensing data. *Forestry: An International Journal of Forest Research* 2022:cpac015.
- Creasy, M. B., W. T. Tinkham, C. M. Hoffman, and J. C. Vogeler. 2021. Potential for individual tree monitoring in ponderosa pine dominated forests using unmanned aerial system structure from motion point clouds. *Canadian Journal of Forest Research* 51:1093–1105.
- Cruz, M. G., M. E. Alexander, and R. H. Wakimoto. 2005. Development and testing of models for predicting crown fire rate of spread in conifer forest stands. *Canadian Journal of Forest Research* 35:1626–1639.
- Dalponte, M., and D. A. Coomes. 2016. Tree-centric mapping of forest carbon density from airborne laser scanning and hyperspectral data. *Methods in Ecology and Evolution* 7:1236–1245.
- Davis, K. T., S. Z. Dobrowski, P. E. Higuera, Z. A. Holden, T. T. Veblen, M. T. Rother, S. A. Parks, A. Sala, and M. P. Maneta. 2019. Wildfires and climate change push low-elevation forests across a critical climate threshold for tree regeneration. *Proceedings of the National Academy of Sciences* 116:6193–6198.
- Despain, D. G. 1990. Yellowstone vegetation: Consequences of environment and history in a natural setting. Roberts Rinehart, Boulder, CO.
- Dobrowski, S. Z., A. K. Swanson, J. T. Abatzoglou, Z. A. Holden, H. D. Safford, M. K. Schwartz, and D. G. Gavin. 2015. Forest structure and species traits mediate projected recruitment declines in western US tree species. *Global Ecology and Biogeography* 24:917–927.
- Donato, D. C., J. B. Fontaine, and J. L. Campbell. 2016. Burning the legacy? Influence of wildfire reburn on dead wood dynamics in a temperate conifer forest. *Ecosphere* 7:e01341.
- Eidenshink, J., B. Schwind, K. Brewer, Z.-L. Zhu, B. Quayle, and S. Howard. 2007. A project for monitoring trends in burn severity. *Fire Ecology* 3:3–21.
- Fernandez-Figueredo, E. G., A. E. Wilson, and S. R. Rogers. 2022. Commercially available unoccupied aerial systems for monitoring harmful algal blooms: A comparative study. *Limnology and Oceanography: Methods* 20:146–158.
- Franklin, J. F., D. Lindenmayer, J. A. MacMahon, A. McKee, J. Magnuson, D. A. Perry, R. Waide, and D. Foster. 2000. Threads of continuity: There are immense differences between even-aged silvicultural disturbances (especially clearcutting) and natural disturbances, such as windthrow, wildfire, and even volcanic eruptions. *Conservation in Practice* 1:8–17.
- Franklin, J. F., R. J. Mitchell, and B. J. Palik. 2007. Natural disturbance and stand development principles for ecological forestry. USDA Forest Service, Northern Research Station,

- General Technical Report NRS-19, Newton Square, PA.
- Gholz, H. L., C. C. Grier, a. G. Campbell, and a. T. Brown. 1979. Equations for estimating biomass and leaf area of plants in the Pacific Northwest. Oregon State University, Forest Research Laboratory, Research Paper 41, Corvallis, OR.
- Gill, N. S., T. J. Hoecker, and M. G. Turner. 2021. The propagule doesn't fall far from the tree, especially after short-interval, high-severity fire. *Ecology* 102:e03194.
- Goodbody, T. R. H., N. C. Coops, and J. C. White. 2019. Digital Aerial Photogrammetry for updating area-based forest inventories: A review of opportunities, challenges, and future directions. *Current Forestry Reports* 5:55–75.
- Graham, R. T., S. McCaffrey, and T. B. Jain. 2004. Science basis for changing forest structure to modify wildfire behavior and severity. USDA Forest Service, Rocky Mountain Research Station, General Technical Report RMRS-GTR-120, Fort Collins, CO.
- Hanna, P., and D. Kulakowski. 2012. The influences of climate on aspen dieback. *Forest Ecology and Management* 274:91–98.
- Hansen, W. D., and M. G. Turner. 2019. Origins of abrupt change? Postfire subalpine conifer regeneration declines nonlinearly with warming and drying. *Ecological Monographs* 89:e01340.
- Harmon, M. E., J. F. Franklin, F. J. Swanson, P. Sollins, S. V. Gregory, J. D. Lattin, N. H. Anderson, S. P. Cline, N. G. Aumen, J. R. Sedell, G. W. Lienkaemper, K. Cromack, and K. W. Cummins. 1986. Ecology of coarse woody debris in temperate ecosystems. Pages 133–302 in A. MacFadyen and E. D. Ford, editors. *Advances in Ecological Research*. Academic Press, Orlando, FL.
- Harmon, M. E., and J. Sexton. 1996. Guidelines for measurements of woody detritus in forest ecosystems. University of Washington, US LTER Network Office, LTER Network Publication 20, Seattle, WA.
- Harvey, B. J., D. C. Donato, and M. G. Turner. 2016a. High and dry: Post-fire tree seedling establishment in subalpine forests decreases with post-fire drought and large stand-replacing burn patches. *Global Ecology and Biogeography* 25:655–669.
- Harvey, B. J., D. C. Donato, and M. G. Turner. 2016b. Burn me twice, shame on who? Interactions between successive forest fires across a temperate mountain region. *Ecology* 97:2272–2282.
- Hayes, K., and B. Buma. 2021. Effects of short-interval disturbances continue to accumulate, overwhelming variability in local resilience. *Ecosphere* 12:e03379.
- Higuera, P. E., and J. T. Abatzoglou. 2021. Record-setting climate enabled the extraordinary 2020 fire season in the western United States. *Global Change Biology* 27:1–2.
- Higuera, P. E., C. Whitlock, and J. A. Gage. 2011. Linking tree-ring and sediment-charcoal records to reconstruct fire occurrence and area burned in subalpine forests of Yellowstone National Park, USA. *Holocene* 21:327–341.
- Hoecker, T. J., W. D. Hansen, and M. G. Turner. 2020. Topographic position amplifies consequences of short-interval stand-replacing fires on postfire tree establishment in subalpine conifer forests. *Forest Ecology and Management* 478:118523.
- Hoecker, T. J., and M. G. Turner. 2022. A short-interval reburn catalyzes departures from historical structure and composition in a mesic mixed-conifer forest. *Forest Ecology and Management* 504:119814.
- Holling, C. S. 1973. Resilience and stability of ecological systems. *Annual Review of Ecology and Systematics* 4:1–23.

- Hostetler, S., C. Whitlock, B. Shuman, D. Liefert, C. W. Drimal, and S. Bischke. 2021. Greater Yellowstone climate assessment: Past, present, and future climate change in Greater Yellowstone watersheds. Montana State University, Institute on Ecosystems, Bozeman, MT.
- Hunt, E. R., and C. S. T. Daughtry. 2018. What good are unmanned aircraft systems for agricultural remote sensing and precision agriculture? *International Journal of Remote Sensing* 39:5345–5376.
- Hutto, R. L. 1995. Composition of bird communities following stand-replacement fires in Northern Rocky Mountain (U.S.A.) conifer forests. *Conservation Biology* 9:1041–1058.
- Jackson, S. T., J. L. Betancourt, R. K. Booth, and S. T. Gray. 2009. Ecology and the ratchet of events: Climate variability, niche dimensions, and species distributions. *Proceedings of the National Academy of Sciences* 106:19685–19692.
- Johnstone, J. F., C. D. Allen, J. F. Franklin, L. E. Frelich, B. J. Harvey, P. E. Higuera, M. C. Mack, R. K. Meentemeyer, M. R. Metz, G. L. W. Perry, T. Schoennagel, and M. G. Turner. 2016. Changing disturbance regimes, ecological memory, and forest resilience. *Frontiers in Ecology and the Environment* 14:369–378.
- Johnstone, J. F., T. N. Hollingsworth, F. S. Chapin, and M. C. Mack. 2010. Changes in fire regime break the legacy lock on successional trajectories in Alaskan boreal forest. *Global Change Biology* 16:1281–1295.
- Kashian, D. M., M. G. Turner, W. H. Romme, and C. G. Lorimer. 2005. Variability and convergence in stand structural development on a fire-dominated subalpine landscape. *Ecology* 86:643–654.
- Keeley, J. E., G. Ne’eman, and C. J. Fotheringham. 1999. Immaturity risk in a fire-dependent pine. *Journal of Mediterranean Ecology* 1:41–48.
- Ker, M. F. 1984. Biomass equations for seven major Maritimes tree species. Canadian Forestry Service, Maritimes Forest Research Centre, Information Report M-X-148, Fredericton, New Brunswick.
- Lorenz, T. J., K. A. Sullivan, A. v. Bakian, and C. A. Aubry. 2011. Cache-site selection in Clark’s Nutcracker (*Nucifraga columbiana*). *Auk* 128:237–247.
- Mack, M. C., X. J. Walker, J. F. Johnstone, H. D. Alexander, A. M. Melvin, M. Jean, and S. N. Miller. 2021. Carbon loss from boreal forest wildfires offset by increased dominance of deciduous trees. *Science* 372:280–283.
- Manfreda, S., M. F. McCabe, P. E. Miller, R. Lucas, V. P. Madrigal, G. Mallinis, E. Ben Dor, D. Helman, L. Estes, G. Ciraolo, J. Müllerová, F. Tauro, M. I. de Lima, J. L. M. P. de Lima, A. Maltese, F. Frances, K. Caylor, M. Kohv, M. Perks, G. Ruiz-Pérez, Z. Su, G. Vico, and B. Toth. 2018. On the use of unmanned aerial systems for environmental monitoring. *Remote Sensing* 10:641.
- McCaughey, W. W., and W. C. Schmidt. 1987. Seed dispersal of Engelmann spruce in the intermountain west. *Northwest Science* 61:1–6.
- McElduff, F., M. Cortina-Borja, S. K. Chan, and A. Wade. 2010. When t-tests or Wilcoxon-Mann-Whitney tests won’t do. *American Journal of Physiology - Advances in Physiology Education* 34:128–133.
- Means, J. E., O. N. Krankina, H. Jiang, and H. Li. 1996. Estimating live fuels for shrubs and herbs with BIOPAK. USDA Forest Service, Pacific Northwest Research Station, Gen. Tech. Rep. PNW-GTR-372, Portland, OR.
- Nelson, K. N., M. G. Turner, W. H. Romme, and D. B. Tinker. 2016. Landscape variation in tree

- regeneration and snag fall drive fuel loads in 24-year old post-fire lodgepole pine forests. *Ecological Applications* 26:2422–2436.
- Nelson, K. N., M. G. Turner, W. H. Romme, and D. B. Tinker. 2017. Simulated fire behaviour in young, postfire lodgepole pine forests. *International Journal of Wildland Fire* 26:852–865.
- Parks, S. A., L. M. Holsinger, C. Miller, and C. R. Nelson. 2015. Wildland fire as a self-regulating mechanism: The role of previous burns and weather in limiting fire progression. *Ecological Applications* 25:1478–1492.
- Parks, S. A., C. Miller, C. R. Nelson, and Z. A. Holden. 2014. Previous fires moderate burn severity of subsequent wildland fires in two large western US wilderness Areas. *Ecosystems* 17:29–42.
- Pausas, J. G., and J. E. Keeley. 2014. Evolutionary ecology of resprouting and seeding in fire-prone ecosystems. *New Phytologist* 204:55–65.
- Prichard, S. J., C. S. Stevens-Rumann, and P. F. Hessburg. 2017. Tamm Review: Shifting global fire regimes: Lessons from reburns and research needs. *Forest Ecology and Management* 396:217–233.
- R Core Team. 2022. R: A language and environment for statistical computing. Vienna, Austria.
- Ratajczak, Z., S. R. Carpenter, A. R. Ives, C. J. Kucharik, T. Ramiadantsoa, M. A. Stegner, J. W. Williams, J. Zhang, and M. G. Turner. 2018. Abrupt change in ecological systems: Inference and diagnosis. *Trends in Ecology and Evolution* 33:513–526.
- Rogers, P. C., B. D. Pinno, J. Šebesta, B. R. Albrechtsen, G. Li, N. Ivanova, A. Kusbach, T. Kuuluvainen, S. M. Landhäusser, H. Liu, T. Myking, P. Pulkkinen, Z. Wen, and D. Kulakowski. 2020. A global view of aspen: Conservation science for widespread keystone systems. *Global Ecology and Conservation* 21:e00828.
- Romme, W. H., and D. G. Despain. 1989. Historical perspective on the Yellowstone fires of 1988. *BioScience* 39:695–699.
- Romme, W. H., and M. G. Turner. 2015. Ecological implications of climate change in Yellowstone: Moving into uncharted territory? *Yellowstone Science* 23:6–13.
- Roussel, J. R., D. Auty, N. C. Coops, P. Tompalski, T. R. H. Goodbody, A. S. Meador, J. F. Bourdon, F. de Boissieu, and A. Achim. 2020. lidR: An R package for analysis of Airborne Laser Scanning (ALS) data. *Remote Sensing of Environment* 251:112061.
- Scheffer, M., and S. R. Carpenter. 2003. Catastrophic regime shifts in ecosystems: Linking theory to observation. *Trends in Ecology and Evolution* 18:648–656.
- Schoennagel, T., M. G. Turner, and W. H. Romme. 2003. The influence of fire interval and serotiny on postfire lodgepole pine density in Yellowstone National Park. *Ecology* 84:2967–2978.
- Schoennagel, T., D. M. Waller, M. G. Turner, and W. H. Romme. 2004. The effect of fire interval on post-fire understorey communities in Yellowstone National Park. *Journal of Vegetation Science* 15:797–806.
- Senf, C. 2022. Seeing the system from above: The use and potential of remote sensing for studying ecosystem dynamics. *Ecosystems* 2022:s10021-022-00777-2.
- Sikkink, P. G., and R. E. Keane. 2012. Predicting fire severity using surface fuels and moisture. USDA Forest Service, Rocky Mountain Research Station, Research Paper RMRS-RP-96, Fort Collins, CO.
- Stevens-Rumann, C. S., A. T. Hudak, P. Morgan, A. Arnold, and E. K. Strand. 2020. Fuel dynamics following wildfire in US Northern Rockies forests. *Frontiers in Forests and Global Change* 3:51.

- Stevens-Rumann, C. S., K. B. Kemp, P. E. Higuera, B. J. Harvey, M. T. Rother, D. C. Donato, P. Morgan, and T. T. Veblen. 2018. Evidence for declining forest resilience to wildfires under climate change. *Ecology Letters* 21:243–252.
- Stevens-Rumann, C. S., and P. Morgan. 2019. Tree regeneration following wildfires in the western US: A review. *Fire Ecology* 15:15.
- Stevens-Rumann, C. S., S. J. Prichard, E. K. Strand, and P. Morgan. 2016. Prior wildfires influence burn severity of subsequent large fires. *Canadian Journal of Forest Research* 46:1375–1385.
- Ter-Mikaelian, M. T., and M. D. Korzukhin. 1997. Biomass equations for sixty-five North American tree species. *Forest Ecology and Management* 97:1–24.
- Tinker, D. B., W. H. Romme, W. W. Hargrove, R. H. Gardner, and M. G. Turner. 1994. Landscape-scale heterogeneity in lodgepole pine serotiny. *Canadian Journal of Forest Research* 24:897–903.
- Turner, M. G., K. H. Braziunas, W. D. Hansen, and B. J. Harvey. 2019. Short-interval severe fire erodes the resilience of subalpine lodgepole pine forests. *Proceedings of the National Academy of Sciences* 116:11319–11328.
- Turner, M. G., K. H. Braziunas, W. D. Hansen, T. J. Hoecker, W. Rammer, Z. Ratajczak, A. L. Westerling, and R. Seidl. 2021. The magnitude, direction, and tempo of forest change in Greater Yellowstone in a warmer world with more fire. *Ecological Monographs*:e01485.
- Turner, M. G., W. H. Romme, and R. H. Gardner. 1999. Prefire heterogeneity, fire severity, and early postfire plant reestablishment in subalpine forests of Yellowstone National Park, Wyoming. *International Journal Of Wildland Fire* 9:21–36.
- Turner, M. G., W. H. Romme, R. A. Reed, and G. A. Tuskan. 2003. Post-fire aspen seedling recruitment across the Yellowstone (USA) landscape. *Landscape Ecology* 18:127–140.
- Turner, M. G., D. B. Tinker, W. H. Romme, D. M. Kashian, and C. M. Litton. 2004. Landscape patterns of sapling density, leaf area, and aboveground net primary production in postfire lodgepole pine forests, Yellowstone National Park (USA). *Ecosystems* 7:751–775.
- Wallace, L., A. Lucieer, Z. Malenovský, D. Turner, and P. Vopěnka. 2016. Assessment of forest structure using two UAV techniques: A comparison of airborne laser scanning and structure from motion (SfM) point clouds. *Forests* 7:62.
- Westerling, A. L. 2016. Increasing western US forest wildfire activity: Sensitivity to changes in the timing of spring. *Philosophical Transactions of the Royal Society B: Biological Sciences* 371:20150178.
- Westerling, A. L., M. G. Turner, E. A. H. Smithwick, W. H. Romme, and M. G. Ryan. 2011. Continued warming could transform Greater Yellowstone fire regimes by mid-21st century. *Proceedings of the National Academy of Sciences* 108:13165–13170.
- Western Regional Climate Center (WRCC). 2021. Old Faithful, Wyoming (486845) NCDC 1981–2010 Monthly Normals. (Accessed 2021-03-11). <https://wrcc.dri.edu/cgi-bin/cliMAIN.pl?wy6845>.
- Whitlock, C., J. Marlon, C. Briles, A. Brunelle, C. Long, and P. Bartlein. 2008. Long-term relations among fire, fuel, and climate in the north-western US based on lake-sediment studies. *International Journal of Wildland Fire* 17:72–83.
- Whitman, E., M. A. Parisien, D. K. Thompson, and M. D. Flannigan. 2019. Short-interval wildfire and drought overwhelm boreal forest resilience. *Scientific Reports* 9:18796.
- Yellowstone National Park (YNP). 2017. Yellowstone resources and issues handbook: 2017. Yellowstone National Park, WY.

Appendix A: Contact Information for Key Project Personnel

Kristin H. Braziunas (student PI), kristin.braziunas@tum.de

Ecosystem Dynamics and Forest Management Group, School of Life Sciences, Technical University of Munich, 85354 Freising, Germany

Monica G. Turner (PI), turnermg@wisc.edu

Department of Integrative Biology, University of Wisconsin-Madison, Madison, WI 53706

Appendix B: Completed/Planned Science Delivery Products

Articles in peer-reviewed journals

Braziunas, K. H., N. G. Kiel, and M. G. Turner. In review. Less fuel for the next fire? Warmer-drier climate amplifies effects of short-interval fire on forest recovery. *Ecology*.

Kiel, N. G., K. H. Braziunas, and M. G. Turner. In prep. Peeking under the canopy: effects of short fire-return intervals on herbaceous understories of Greater Yellowstone.

Graduate dissertation

Braziunas, K. H. 2021. Operationalizing resilience of social-ecological systems to changing climate and fire in US Northern Rocky Mountain forests. PhD Dissertation. University of Wisconsin-Madison.

Oral presentations and webinars

Braziunas, K. H. and T. J. Hoecker. Lessons from reburns in Greater Yellowstone and Glacier. Northern Rockies Fire Science Network Webinar. Planned for March 15, 2023.

Braziunas, K. H. Anticipating future forests: Resilience, risk, and ecosystem services under changing climate and fire. Ecology and Evolutionary Biology Seminar, Division of Biology, Kansas State University. March 2022.

Braziunas, K. H. Operationalizing resilience of social-ecological systems to changing climate and fire in US Northern Rocky Mountain forests. PhD Exit Seminar, Integrative Biology, University of Wisconsin-Madison. December 2021.

Braziunas, K. H. Sources of ignition: Becoming a fire ecologist. 2 invited talks, Philanthropic Educational Organization (P.E.O.) Madison Chapter DH, Madison Chapter DV. March-April 2021.

Kiel, N. G., K. H. Braziunas, and M. G. Turner. 2022. Peeking under the canopy: effects of short fire-return intervals on herbaceous understories in Greater Yellowstone. (Oral presentation). Biennial Scientific Conference on the Greater Yellowstone Ecosystem, Bozeman, Montana, May 15-18.

Kiel, N. G., K. H. Braziunas, and M. G. Turner. 2022. Peeking under the canopy: effects of short fire-return intervals on herbaceous understories in Greater Yellowstone. (Oral presentation). UW-Madison Center for Ecology and the Environment's Spring Symposium, Madison, Wisconsin, May 2-3.

Kiel, N. G. 2022. Peeking under the canopy: climate, fire, and Greater Yellowstone plant communities. Public talk (virtual), Teton Chapter, Wyoming Native Plants Society, Jackson, Wyoming.

Selected media coverage and outreach

McKinney, Holly. Researcher in the Park. Grand Teton National Park and John D. Rockefeller Memorial Parkway: Vital Signs 2020. (<https://www.nps.gov/grte/learn/nature/upload/2020-GRTE-Vital-Signs-Web-access-final.pdf>)

Field tour for Superintendent and leadership team of Grand Teton National Park, led by M. G. Turner. July 11, 2022.

Code for reproducing analyses

Braziunas, K. H. Code associated with Less fuel for the next fire? Warmer-drier climate amplifies effects of short-interval fire on forest recovery. Currently available for peer reviewers (https://github.com/kbraziun/Braziunas_etal_SILI).

Braziunas, K. H. Code for reproducing R analysis deriving forest structure from UAS point clouds. (<https://github.com/kbraziun/PointCloudProcessing>)

Appendix C: Metadata

Newly collected field data and associated metadata will be deposited upon manuscript acceptance at the Environmental Data Initiative. Data will be described and documented in accordance with the Ecological Metadata Language standard, and the dataset will be assigned a permanent, unique URL and DOI. The original Data Management Plan stated that data would be deposited with the USDA Forest Service Research Data Archive; instead, we will cross-list the deposited data in this archive.

Processed point clouds derived from UAS DAP are available, along with additional post-processing code, on Github (<https://github.com/kbrazuun/PointCloudProcessing>).

Appendix D: Supplemental Tables

Table D1. Presence (proportion of plots) and stem density (stems ha⁻¹) by species in long- and short-interval plots ($n = 33$ of each).

Species	Presence Proportion		Test statistic	p	Stem density		Test statistic	p
	Long	Short			Mean (SE) Range	Long		
ABLA	0.27	0.21	0.77	0.45	97 (53) 0-1667	13 (6) 0-167	-7.45	2×10⁻⁸
PIAL	0.18	0.09	1.74	0.09	77 (40) 0-1133	20 (14) 0-433	-2.26	0.03
PICO	1.00	1.00	—	—	28189 (9560) 33-197433	2790 (663) 25-14825	490	7×10⁻⁵
PIEN	0.42	0.30	1.42	0.16	286 (174) 0-5667	23 (10) 0-300	-8.14	3×10⁻⁹
POTR	0.24	0.36	-1.60	0.12	62 (37) 0-1200	384 (164) 0-4300	3.16	0.003
PSME	0.24	0.09	1.86	0.07	31 (13) 0-267	10 (8) 0-267	-0.22	0.83

Note: Differences in lodgepole pine density were tested with a two-sided, paired Wilcoxon signed rank test (test statistic = V). Presence and density for all other species were tested with zero-inflated negative binomial regression models adjusted for matched data (test statistic = t, df = $n - 1$). Abbreviations: ABLA: Subalpine fir, PIAL: Whitebark pine, PICO: Lodgepole pine, PIEN: Engelmann spruce, POTR: Quaking aspen, PSME: Douglas-fir.

Table D2. Canopy and surface fuel and biomass pools in long- and short-interval plots ($n = 22$ each of short and long plots unless otherwise noted); due to time constraints, fuels data were not measured in one plot pair and shrubs were not measured in two plot pairs.

Biomass or fuel characteristic	Long interval	Short interval	Test or trans.	Test statistic	p
	Mean (SE) Min-Max	Mean (SE) Min-Max			
Live tree aboveground (all species)	10.25 (4.01) 0-63.64	1.46 (0.70) 0-15.32	—	—	—
<i>Canopy fuels (conifers only)</i>					
Available canopy fuel load	3.57 (1.39) 0-23.71	0.52 (0.26) 0-5.62	—	—	—
Canopy bulk density (kg m ⁻³)	0.20 (0.10) 0-2.14	0.03 (0.01) 0-0.30	—	—	—
<i>Dead aerial fuels</i>					
1-h snag size class	—	0.00 (0.00) 0-0.01	—	—	—
10-h snag size class	0.01 (0.00) 0-0.10	0.29 (0.21) 0-4.50	—	—	—

Biomass or fuel characteristic	Long interval Mean (SE) Min-Max	Short interval Mean (SE) Min-Max	Test or trans.	Test statistic	p
100-h snag size class	0.41 (0.20) 0-4.48	1.98 (0.72) 0-13.36	Wilcoxon	48	0.11
1000-h snag size class	53.88 (8.41) 0-133.92	3.19 (0.98) 0-18.78	Cube root	9.81	3×10⁻⁹
Total snag	54.29 (8.41) 0-134.16	5.46 (1.28) 0-20.45	Square root	9.03	1×10⁻⁸
<i>Live surface fuels</i>					
Sapling aboveground (lodgepole pine)	2.40 (1.54) 0-34.18	0.19 (0.06) 0-0.93	Wilcoxon	214	0.003
Shrub (<i>n</i> = 20)	0.08 (0.01) 0.01-0.22	0.08 (0.02) 0-0.46	Cube root	0.70	0.49
<i>Dead surface fuels (n = 21)</i>					
Litter	3.84 (0.80) 0.03-16.20	2.62 (0.66) 0.17-11.41	Wilcoxon	168	0.07
Duff	12.01 (2.46) 0-45.52	9.14 (2.54) 0-45.34	Wilcoxon	110	0.12
1-h	0.16 (0.04) 0.01-0.72	0.10 (0.02) 0-0.34	Wilcoxon	162	0.11
10-h	1.68 (0.26) 0.09-5.02	1.37 (0.25) 0-4.42	No trans.	0.79	0.44
100-h	3.66 (0.52) 1.00-11.98	4.86 (0.68) 1.21-12.79	Wilcoxon	58	0.08
Sound 1000-h	45.86 (7.73) 5.67-154.30	32.10 (6.59) 0-105.30	Wilcoxon	151	0.23
Rotten 1000-h	17.64 (5.53) 0-95.75	16.14 (2.92) 0.31-56.92	Cube root	-1.29	0.21
Total live aboveground (tree + sapling + shrub)	12.73 (4.98) 0.06-91.14	1.72 (0.73) 0.02-16.27	Log10	3.82	0.0005
Total dead woody (snags + downed wood, <i>n</i> = 21)	121.25 (7.92) 58.97-203.50	60.19 (7.80) 20.15-153.54	No trans.	7.48	2×10⁻⁷

Note: All loads are in Mg ha⁻¹ unless otherwise noted. Differences between plot pairs were tested with one-sided, paired t-tests (total live and total dead, test statistic = *t*), two-sided paired t-tests (test statistic = *t*, *df* = *n* - 1), or Wilcoxon signed rank tests (test statistic = *V*). The Test or transformation (trans.) column indicates whether a Wilcoxon test was used or whether a transformation was used with a t-test (No trans. = data was not transformed).